



Published in final edited form as:

Biogerontology. 2009 April ; 10(2): 125–151. doi:10.1007/s10522-008-9157-3.

Genomic and proteomic profiling of oxidative stress response in human diploid fibroblasts

Lifang Xie

Department of Pharmacology, College of Medicine, University of Arizona, 1501 N. Campbell Ave., Tucson, AZ 85724, USA

Ritu Pandey

Bioinformatics Core, Arizona Cancer Center, Tucson, AZ 85724, USA

Beibei Xu

Department of Pharmacology, College of Medicine, University of Arizona, 1501 N. Campbell Ave., Tucson, AZ 85724, USA

George Tsaprailis

Proteomics Core Facility, Southwest Environmental Health Sciences Center, Tucson, AZ 85721, USA

Qin M. Chen

Department of Pharmacology, College of Medicine, University of Arizona, 1501 N. Campbell Ave., Tucson, AZ 85724, USA

Abstract

A number of lines of evidence suggest that senescence of normal human diploid fibroblasts (HDFs) in culture is relevant to the process of aging in vivo. Using normal human skin diploid fibroblasts, we examine the changes in genes and proteins following treatment with a mild dose of H₂O₂, which induces premature senescence. Multidimensional Protein Identification Technology (MudPIT) in combination with mass spectrometry analyses of whole cell lysates from HDFs detected 65 proteins in control group, 48 proteins in H₂O₂-treated cells and 109 proteins common in both groups. In contrast, cDNA microarray analyses show 173 genes up-regulated and 179 genes down-regulated upon H₂O₂ treatment. Both MudPIT and cDNA microarray analyses indicate that H₂O₂ treatment caused elevated levels of thioredoxin reductase 1. Semi-quantitative RT-PCR and Western-blot were able to verify the finding. Out of a large number of genes or proteins detected, only a small fraction shows the overlap between the outcomes of microarray versus proteomics. The low overlap suggests the importance of considering proteins instead of transcripts when investigating the gene expression profile altered by oxidative stress.

Keywords

Oxidative stress; Human diploid fibroblasts; Senescence; Gene expression; Proteomics

Introduction

Oxidative stress has been linked to aging and many aging associated diseases. While increased levels of oxidative biomarkers can be detected in aging population, oxidants are produced by endogenous sources, such as mitochondrial respiration, which generates reactive oxygen species (ROS) as byproducts. Increased production of oxidants results from saturation of antioxidant defenses, such as inactivation of antioxidant enzymes and depletion of sulfhydryls due to nutritional imbalance or exposure to xenobiotics. Under most circumstances, the level of oxidants produced endogenously is relatively low and not sufficient to kill the majority of cells. However oxidative damage can accumulate over time, such as during the process of aging, and contribute to senescence at the cellular level and consequently functional decline. Despite of the fact that oxidative stress is known to be associated with aging and aging associated diseases, epidemiological studies and clinical trials with antioxidant vitamins have generated conflicting data. These controversies argue for the importance of understanding the molecular mechanism underlying oxidative stress.

Recent development in genomic and proteomic technologies provides an opportunity to study the biology of oxidative stress systematically. Microarray technologies allow the examination of gene expression on the scale of a genome when an organism or cells experience a changing status. Several laboratories have utilized the technology for uncovering changes of gene expression associated with aging, replicative senescence or oxidant induced premature senescence (de Magalhaes et al. 2004; Lee et al. 1999; Pascal et al. 2007; Shelton et al. 1999). However, despite of the advancement in microarray technologies, the question remains unanswered as how many genes showing changes at the mRNA level also change their expression at the protein level. Complementary technologies, such as LC-MS/MS based proteomics, provide an opportunity to profile for proteins appearing with different states of cells. Since proteins ultimately depict the function of genes, it is important to reveal the identities of the proteins showing changes with oxidative stress.

Multidimensional chromatography coupled with mass spectrometry is an emerging technique for profiling proteins in a complex mixture. To improve the resolution for LC-MS/MS based proteomics, Multidimensional Protein Identification Technology (MudPIT) employs biphasic or triphasic micro-capillary columns for high-performance liquid chromatography (Florens and Washburn 2006; Paoletti et al. 2004; Washburn et al. 2001; Wolters et al. 2001). With tandem mass spectrometer, peptides eluted from liquid chromatography can be identified in combination with sequence database searching tools. Although technology improvement remains as a main focus of proteomics, current MudPIT and mass spectrometry based techniques have shown promise in finding new targets and new pathways by profiling proteins in a complex mixture such as biological fluids, tissue extracts, cell lysates, and subcellular organelles (Breci and Haynes 2007; Chen et al. 2006; Kislinger et al. 2005; Mauri et al. 2005; Washburn et al. 2001). These techniques allow us to profile changes at the protein level when cells experience oxidative stress.

Fibroblasts are the most abundant cell types within our body. Normal human diploid fibroblasts (HDFs) can be isolated from certain tissues, for example the skin, and remain

viable under tissue culture condition. Unlike human tumor cells or immortalized rodent cells, HDFs have a limited replicative potential in culture (Campisi and d'Adda di Fagagna 2007; Cristofalo et al. 2004; Hayflick and Moorhead 1961). Fibroblasts from the foreskin of newborns generally replicate 50 – 80 population doublings before reaching replicative senescence. On the other hand, early passage of HDFs develop a phenotype resembling premature senescence following the exposure to low or mild dose of oxidants (Chen and Ames 1994; Chen et al. 2000a, c, 2001; Chen 2000). Differing from tumor cells, HDFs from individuals with normal genetic background retain genomic integrity in culture, allowing us to profile changes relevant to human health as a whole. In this study, we compare the outcome of proteomics with that of microarray using current available technologies after stressing HDFs with a mild dose of H₂O₂.

Materials and methods

Chemicals and reagents

Chemicals were purchased from Sigma unless otherwise indicated. Stabilized H₂O₂ (H-1009, Sigma) was used and the concentration of the stock was verified by absorbency at 240 nm.

Maintenance of cell culture and treatment with H₂O₂

HCA₃ human dermal fibroblasts were obtained from Dr. Olivia Pereira-Smith at the population doubling level (PDL) 20. These cells typically reach replicative senescence after PDL 80 and were used for this study at PDL 26–40. Stock HCA₃ cells were subcultured weekly in 10 ml of Dulbecco's modified Eagle's medium (DMEM) containing 10% (v/v) fetal bovine serum, 50 units/ml penicillin, and 50 µg/ml streptomycin (Invitrogen) at a seeding density of 1 ± 10^6 cells/100-mm Falcon dish. For H₂O₂ treatment, cells were seeded at a density of 2 ± 10^6 /100-mm dish. In 5 days, cells have reached confluence with the density of $10.48 \pm 0.85 \pm 10^6$ cells per 100-mm dish, and were treated with 600 µM H₂O₂ in a 100-mm dish containing 10 ml of medium. After 2-h incubation in the presence of H₂O₂, cells were placed in fresh DMEM containing 10% (v/v) FBS and were allowed to recover for 3 days before harvesting RNA or proteins.

MudPIT and LC-MS/MS analysis of cell lysates

Cells were harvested in 200 µl of EB lysis buffer (Coronella-Wood et al. 2004). Each sample was diluted by and dialyzed against 0.01 N NH₄HCO₃, passed through a 0.45-µm filter to remove insoluble cell debris, and concentrated down using a speed vacuum concentrator. After protein concentration determination by the Bradford method (Bio-Rad, Hercules, CA), protein mixtures from whole cell lysates were digested overnight with trypsin at a 50:1 ratio (Xie et al. 2005). A microbore HPLC system (Paradigm MS4, Michrom, Auburn, CA) was used with two separation columns: a reverse phase (RP) column and a strong cation exchange (SCX) column (Whatman, Clifton, NJ). The sample (23 µg) was acidified using TFA and injected onto the SCX column, with the effluents going through RP column. A twelve-step fractionation analysis was performed with the solvents of: 10% methanol/0.1% formic acid, 0.01% TFA (buffer A), 95% methanol/0.1% formic acid, 0.01% TFA (buffer B), 10% methanol/0.1% formic acid, 0.01% TFA (buffer C) and 500 mM ammonium

acetate/10% methanol/0.1% formic acid, 0.01% TFA (buffer D). Eluted peptides were electrosprayed into the mass spectrometer with a distally applied liquid junction spray voltage of 1.6 kV. Spectra are scanned over the range 380–2000 mass units. Automated peak recognition, dynamic exclusion, and daughter ion scanning of the most intense ion was performed using the Xcalibur software (Andon et al. 2002).

cDNA Microarray analysis

The microarray chips were generated as described by Watts et al. (2001). The chips contain ~5300 human genes, with more than 3000 known genes and the remainders as expressed sequence tags (ESTs) determined by the UniGene (<ftp://azccftp.arizona.edu/gwatts/GeneList/>). Microarray analyses were performed as described by Crowley-Weber et al. (2002). Briefly, total RNAs were isolated using a QIAGEN RNeasy kit (Qiagen, Valencia, CA). Cy3 or Cy5 labeled first strand cDNAs were made from 40 µg of total RNA with Micromax Direct cDNA Microarray System (NEN Life Sciences, Boston, MA). Fluorescence labeled cDNAs from two reactions were hybridized to the cDNA array slides for scanning with Axon GenePix 4000 microarray reader (Axon Instruments, Foster City, CA) and quantification with GenePix software. The data were analyzed with GeneSpring 5.0 software (Silicon Genetics, Redwood, CA).

Three independent experiments were performed with cells from three different passages. Each experiment has triplicate hybridizations. Changes in gene expression are judged by 1.5 fold or greater difference in Cy5 versus Cy3 signal strength and a *P*-value of <0.05 in a paired *t*-test among the triplicates. The up- versus down-regulated genes were classified and clustered by searching through the BioRag database generated by the Arizona Cancer Center Bioinformatics Core (www.biorag.org) and categorization was verified individually by Unigene database search. If a gene encodes a protein with multiple functions, it is placed under the category of its most recognized function.

Functional analysis and gene ontology networks

Cytoscape 2.4.0 (www.cytoscape.org) was used to generate the network of Gene Ontology (GO) terms (Purdom-Dickinson et al. 2007). Differentially expressed genes and proteins found by cDNA microarray and LC-MS/MS based proteomics analyses were searched against BioRag database (www.biorag.org) for GO Molecular Function categories. The categories that had less than four genes were removed if the genes were also not represented in any other molecular function categories for microarray data. For proteomic data, all the proteins found different between control versus treated groups and their GO categories were included for generating the network. The categories containing only one gene were removed. Individual gene or protein is presented as a circular node with GO terms appearing as squares. The edges show the links between the genes/proteins versus the GO terms. The color shade in circular node reflects the fold change for up regulated (red) and down regulated (blue) genes for the network constructed from gene expression arrays. For the protein network, the node color indicates proteins found in control (green) or in H₂O₂ treated cells (red).

Semiquantitative RT-PCR

Total RNA was extracted from cells with TRIZOL (Invitrogen) for reverse transcription (2 µg RNA/sample) and PCR (3 µl of the 35 µl RT reaction mixture). Glyceraldehyde-3-phosphate dehydrogenase (GAPDH) was used as a reference gene for internal loading control. The Primer 3 Input Program (<http://frodo.wi.mit.edu/cgi-bin/primer3/primer3.cgi>) was used to design PCR primers and to calculate the optimal PCR annealing temperature (TempA, Table 1). PCR products were detected by ethidium bromide staining after agarose gel electrophoresis.

Western blot analysis

Cells were scraped in 200 µl of EB lysis buffer and proteins (40 µg) from cell lysates were separated by 15% SDS-polyacrylamide gel electrophoresis before overnight transfer to a polyvinylidene difluoride (PVDF) membrane (Millipore, Bedford, MA). The protein bound to PVDF membrane was detected by overnight incubation at 4°C in the antibody against AURKA (1:2000 dilution, rabbit polyclonal, ab12324, abcam, MA), MMP-3 (1:2000 dilution, mouse monoclonal, MAB3306, Chemicon, CA), TXN (1:1000 dilution, mouse monoclonal, ab16965, abcam, MA), TXNRD1 (1:1000 dilution, rabbit polyclonal, 07-613, Upstate, NY), p53 (1:100, rabbit polyclonal, sc-6243, Santa Cruz Biotechnology), p21 (1:200, mouse monoclonal, #556431, Pharmingen BD), and p16 (1:200, mouse monoclonal, #554070, Pharmingen BD), or GAPDH (1:2000 dilution; rabbit polyclonal, ab9485-100, Abcam, MA). Bound antibody was recognized by horseradish peroxidase-conjugated secondary antibodies (Zymed Laboratories Inc., South San Francisco, CA; 1:8000) for enhanced chemiluminescence (ECL) reaction.

Results

Identification of proteins in cell lysates by LC-MS/MS

Previous works from our laboratory have shown that H₂O₂ at the dose less than 0.85 pmol/cell appears to be non-lethal and induces premature senescence over a course of 7 days in early passage HDFs (Chen and Ames 1994; Chen et al. 2000a, c, 2001; Chen 2000). In this study, confluent cultures of HCA3 cells were treated with 600 µM H₂O₂. This dose is equivalent to ~0.6 pmol of H₂O₂/cell. The treatment caused all cells to stop DNA synthesis as measured by bromodeoxyuridine incorporation and about 70% cells express Senescent Associated β-galactosidase (SA β-gal) at the time of sample harvesting, i.e. 3 days after H₂O₂ treatment. The ratio of β-gal positive cells will increase if the cells were kept for longer period of time, typically 7 days when senescent morphology and markers are showing in full (Chen et al. 2000b). Cell lysates were collected from Control (Ctrl) and H₂O₂ treated cells for MudPIT and mass spectrometry analyses.

A representative Total Ion Current (TIC) chromatogram from control or H₂O₂ treated cells is shown in Fig. 1. MS/MS data were analyzed using Turbo SEQUEST against a non-redundant human protein sequence database from NCBI (Eng et al. 1994; Link et al. 1999). The criteria for a positive peptide identification for a doubly-charged peptide are a correlation factor (Xcorr) greater than 2.5, a delta cross-correlation factor (ΔXcorr) greater than 0.08, a minimum of one tryptic peptide terminus, and a high preliminary scoring. For

triply- and singly-charged peptides, the Xcorr threshold is set at 3.5 and 1.8, respectively. In all cases, the value of Ions is greater than 50%. SEQUEST outputs were assembled and filtered into actual protein identifications by the DTASelect algorithm (Tabb et al. 2002).

The analyses found 109 proteins common among Ctrl and H₂O₂ treated HDFs (data not shown). There are 65 proteins appearing to Ctrl group only and 48 proteins appearing to H₂O₂ treated HDFs only (Table 2). The network of changes in the proteins is shown in Fig. 2. A cluster of metal ion binding proteins and several proteins in the oxidoreductase cluster have been found in H₂O₂ treated cells (Table 2 and Fig. 2a). Among the proteins not detected in H₂O₂ treated cells, the clusters of protein binding, RNA binding and structural constituents of ribosome stand out (Fig. 2b).

TXN and TXNRD1 are two examples of proteins found in H₂O₂ treated cells. The MS/MS spectra and SEQUEST Flicka protein information output on TXN and TXNRD1 are shown in Figs. 3 and 4. Three peptides were identified from TXN protein by our mass spectrometer (Fig. 3a–c). These peptides cover 37.1% of entire TXN protein sequence (Fig. 3d). The high percentage of sequence coverage, together with the acceptable Xcorr and Ions values give us the confidence in identification of this protein. Unlike TXN, the mass spectrometer only detected one peptide ion for TXNRD1 (Fig. 4a). However, the MS/MS spectrum (Fig. 4a), Xcorr value (3.11 for +2 ion) and Ions scores (67.9%) all suggest the high confidence of this protein identification. Western blot analyses were able to verify elevated levels of TXN and TXNRD1 with H₂O₂ treated HDFs (Fig. 5). At the same time point, the proteins encoding p21 cyclin dependent kinase inhibitor or p53 tumor suppressor also show elevations (Fig. 5). Unlike replicative senescent cells, H₂O₂ induced premature senescence does not cause elevation of the p16 cyclin dependent kinase inhibitor (Fig. 5). These data suggest that H₂O₂ treated cells indeed elevate protein levels of TXN and TXNRD1.

Alterations of gene expression profiles in HDFs upon H₂O₂ treatment

Microarray technology was adopted to address whether the proteins found differentially expressed between control and H₂O₂ treated cells show changes at the mRNA level. With RNA samples collected from Ctrl and H₂O₂ treated HDFs, we measured changes in gene expression by quantifying the binding of Cy5 versus Cy3 labeled cDNA to complementary strands of DNA immobilized onto a microscopic chip. To test whether the genes detected by proteomics also show changes at mRNA level by any chance, we used less stringent selection criteria by counting for the genes showing 1.5-fold or more changes in two out of three independent experiments, each of which has triplicates in hybridization. We found that 173 genes were up-regulated and 179 genes were down regulated by H₂O₂ treatment.

Functional genomics using BioRag program classified 17 up-regulated genes as related to oxidoreductase, antioxidant and detoxification responses (Table 3). These 17 genes are TXNRD1, Glutamate-cysteine ligase modifier subunit (GCLM), glutathione peroxidase 1 (GPX1), glutathione synthetase (GSS), type II hydroxyacyl-Coenzyme A dehydrogenase (HADH2), lysyl oxidase (LOX), NADP + dependent methylenetetrahydrofolate dehydrogenase 2 (MTHFD2), alpha N-acetylglucosaminidase (NAGLU), prostaglandin endoperoxide synthase 1 (PTGS1), prostaglandin endoperoxide synthase 2 (PTGS2) and 7 genes encoding different isoforms of metallothioneins (MTs), i.e. MT1A, MT1E, MT1G,

MT1H, MT1M, MT1X and MT2A. Altered proteases, signaling molecules, kinases, and transcription regulators also stand out as a characteristic of H₂O₂ treated cells (Table 3). In addition, H₂O₂ treatment caused elevated expression of a significant amount of cytokines or chemokines (Table 3).

Cytoscape-based gene network sorting shows a significant portion of upregulated genes in the clusters of oxidoreductase, transferases, metal ion binding, protein Ser/Thr kinase, ATP binding, GTP binding, protein binding, and DNA binding (Fig. 6a). Most of these clusters also contain downregulated genes (Fig. 6b). The clusters showing more decreased than increased genes include receptors and hydrolases (Fig. 6a, b).

Seven of up-regulated genes were chosen randomly for verification using semi-quantitative RT-PCR. With primer sets specific to ADP-ribosylation factor 4-like (ARF4L), Serine/threonine kinase 15 (Aurora kinase A, AURKA), matrix metalloproteinase 3 (MMP3), Small inducible cytokine A7 (CCL7), Small inducible cytokine subfamily A13 (CCL13), Tumor necrosis factor receptor superfamily member 12A (TNFRSF12A), or TXNRD1, RT-PCR with total RNA show increases in the transcripts of these genes by H₂O₂ treatment (Fig. 7).

The overlaps of proteins and transcripts induced by H₂O₂

With the long lists of proteins or genes detected by proteomics or microarray respectively, we have searched for the common outcome between the two platforms of technology. Both LC-MS/MS and cDNA microarray detected the induction of TXNRD1 by H₂O₂ treatment (Tables 2, 3). This finding was confirmed by RT-PCR and Western blot techniques (Figs. 5, 7). Among the decreased genes in H₂O₂ treated cells, A kinase anchor protein 12 and NAD malate dehydrogenase 1 were found common between microarray and proteomic outputs (Tables 2, 3). TXN was found elevated by proteomics but the gene was absent on the microarray chips. RT-PCR analyses show elevated levels of TXN mRNA in H₂O₂ treated cells (Fig. 7). MMP3 and AURKA are among elevated genes detected by microarray analyses in H₂O₂ treated cells. While proteomics failed to detect these two proteins, Western blots found elevated levels of these two proteins in H₂O₂ treated cells (Fig. 8). Adding up together, only a short list of genes was found to increase or decrease by both microarray and proteomics in H₂O₂ treated cells.

Discussion

The proteome often depicts the functional status of cells or an organism. The association of oxidative stress with the process of aging suggests the importance of uncovering the proteome of oxidative stress in studying the biology of aging. The availability of microarray technology has animated the assumption that genes showing increases at the mRNA level are elevated at the protein level. Using current available technologies, we have intended to address the overlap between transcripts and proteins altered by oxidative stress using HDFs as an experimental system. Even with a low stringency data analysis method of microarray, most of the genes showing changes at the protein level in H₂O₂ treated cells were not detected for changes in transcripts by microarray analyses. Only TXNRD1 was detected by both LCMS/MS based proteomics and cDNA microarray technique for elevated expression with H₂O₂ treatment. Two down regulated genes, A kinase anchor protein 12 and NAD

malate dehydrogenase 1, were identified as the overlaps between microarray and proteomics. These results challenge the assumption that genes showing elevation in transcripts are expressed into proteins at higher levels.

Despite of the short list of overlapping genes, transcript or protein network analyses using BioRag and Cytoscape programs point to similar biochemical pathways altered by H₂O₂ treatment. A cluster of genes or proteins has been found related to oxidoreductase, antioxidants and detoxification enzymes. The finding of elevated expression of TXN and TXNRD1 in H₂O₂ treated cells is consistent with previous reports (Mustacich and Powis 2000). TXN and TXNRD1 are downstream target genes of AP-1 and/or Nrf-2 transcription factors, both of which are activated by H₂O₂ (Coronella-Wood et al. 2004; Purdom-Dickinson et al. 2007; Sen and Packer 1996). TXNRD1 belongs to a family of glutathione reductase-like flavoenzymes, a homodimeric selenium-containing protein that catalyzes NADPH-dependent reduction of TXN disulfide (Arner and Holmgren 2000; Becker et al. 2000; Mustacich and Powis 2000). Following oxidative stress, TXNRD1 initiates the reduction and therefore activation of TRX, which relocates from the cytoplasm to the nucleus to turn on the nuclear components of redox-sensitive signaling pathways, for example Ref-1, and activates transcription factors such as AP-1 and NF-κB (Hirota et al. 1997; Karimpour et al. 2002; Schenk et al. 1994; Wei et al. 2000). These transcription factors modulate the expression of downstream target genes important for the gain of repair function against the initial oxidative damage and for development of defense against further insults.

Microarray studies have indicated upregulation of metal binding proteins MTs by H₂O₂ treatment. This finding is consistent with literature reports where MT1A, MT1X, and MT2A have been shown to elevate expression in response to H₂O₂ treatment (Andrews 2000; Dalton et al. 1994; Liu and Thiele 1996; Tate et al. 2002). MTs are characterized by their unusually high content of thiols and are capable of binding to iron and preventing the redox cycling of iron (Kang 2006). As a result, MTs often act as scavengers of ROS, including hydroxyl, phenoxy, and NO radicals (Kang 2006; Sato and Bremner 1993). Most MTs are secreted, which may explain the absence of their detection by proteomics using cell lysates. Nevertheless, MT mediated cytoprotection serves as a redundant mechanism in addition to TXN/TXNRD in cellular adaptation to oxidative stress.

Fibroblasts are capable of producing various paracrine factors such as peptide growth factors, cytokines, and chemokines (Buckley et al. 2001; Smith et al. 1997). We found H₂O₂ treatment caused elevated expression of several cytokines: small inducible cytokine A7 (CCL7), small inducible cytokine subfamily A member 13 (CCL13), CC chemokine CCL28 (CCL28), Interleukin 1 beta (IL1B), Interleukin 32 (IL32), Leukemia inhibitory factor (LIF) and Colony stimulating factor 3 (CSF3). Although many of these genes are among the long list of novel finding of oxidative stress response, elevated expression of cytokines and chemokines, for example Interleukin 1 beta, interleukin 6, and interleukin 15, have been found in microarray studies of replicative senescence (de Magalhaes et al. 2004; Shelton et al. 1999). In addition to cytokines and chemokines, H₂O₂ treated cells expressing MMP3 and IGFBP6. Increased expression of MMP3, i.e. stromelysin-1, and IGFBP-5 has been reported with replicative senescent HDFs (de Magalhaes et al. 2004; Shelton et al. 1999).

Our microarray data add an additional piece of evidence suggesting the similarity between H₂O₂ induced premature senescence and replicative senescence.

Several possibilities explain the short list of overlaps between microarray and proteomics data. The cell lysates used here do not contain secreted proteins, although microarray can detect genes encoding secreted proteins, for example MMP3 and IGFBP6. IGFBP6 was found elevated in H₂O₂ treated HDFs while profiling the secreted proteins (Xie et al. 2005). In addition to the absence of secreted proteins for proteomic detection, we used human 5 K cDNA gene chip for the microarray analyses in this study. Checking the list of genes on these chips, we found that 52% of the proteins detected by LC-MS/MS were absent on the Human 5 K cDNA chip (Table 2). For example, TXN protein was detected in the cell lysate of H₂O₂ treated HDFs by MudPIT analysis but the cDNA sequence of the gene was absent in our microarray slides (Table 2). If we factor in the absence of the genes for 50% detected proteins, the amount of overlapping genes and proteins detected by microarray and proteomics could be at least doubled.

The large gap between the genes expressed at the level of mRNA versus protein may be related to the regulatory mechanism of protein translation under oxidative stress. The process of protein translation is carried by the ribosomes and at least 14 eukaryotic initiation factors (eIFs). About 95–97% genes are translated via 5' methyl cap mechanism (Gebauer and Hentze 2004; Merrick 2004; Preiss and M 2003). This type of translation requires a large quantity of ATP and is generally turned off during stress to conserve energy (Holcik and Sonenberg 2005; Merrick 2004). Only 3–5% genes contain internal ribosomal entry site (IRES), allowing selective protein translation to occur under stress condition (Holcik and Sonenberg 2005; Merrick 2004). Given such a small percentage of genes containing IRES, it is expected that not all the transcripts showing elevated levels are actually translated. Therefore even with improved microarray or proteomic technology, one may find that the overlap between the increases at the level of mRNA versus that of protein remains small.

Acknowledgments

Work in our laboratory has been supported by NIH ES010826, HL076530 and ES007091 (QMC). We thank the Proteomics Facility Core of Southwest Environmental Health Sciences Center (ES06694) for LC-MS/MS analyses, and the Genomics and Bioinformatics facilities supported jointly by the Arizona Cancer Center (P30CA23074) and the Southwest Environmental Health Sciences Center (ES06694) for microarray analyses.

References

- Andon NL, Hollingworth S, Koller A, Greenland AJ, Yates JR 3rd, Haynes PA. Proteomic characterization of wheat amyloplasts using identification of proteins by tandem mass spectrometry. *Proteomics*. 2002; 2:1156–1168. doi:10.1002/1615-9861(200209)2:9<1156 :AID-PROT1156>3.0.CO;2-4. [PubMed: 12362334]
- Andrews GK. Regulation of metallothionein gene expression by oxidative stress and metal ions. *Biochem Pharmacol*. 2000; 59:95–104. doi:10.1016/S0006-2952(99)00301-9. [PubMed: 10605938]
- Arner ES, Holmgren A. Physiological functions of thioredoxin and thioredoxin reductase. *Eur J Biochem*. 2000; 267:6102–6109. doi:10.1046/j.1432-1327.2000.01701.x. [PubMed: 11012661]
- Becker K, Gromer S, Schirmer RH, Muller S. Thioredoxin reductase as a pathophysiological factor and drug target. *Eur J Biochem*. 2000; 267:6118–6125. doi:10.1046/j.1432-1327.2000.01703.x. [PubMed: 11012663]

- Breci L, Haynes PA. Two-dimensional nanoflow liquid chromatography-tandem mass spectrometry of proteins extracted from rice leaves and roots. *Methods Mol Biol.* 2007; 355:249–266. [PubMed: 17093316]
- Buckley CD, Pilling D, Lord JM, Akbar AN, Scheel-Toellner D, Salmon M. Fibroblasts regulate the switch from acute resolving to chronic persistent inflammation. *Trends Immunol.* 2001; 22:199–204. doi:10.1016/S1471-4906(01)01863-4. [PubMed: 11274925]
- Campisi J, d'Adda di Fagagna F. Cellular senescence: when bad things happen to good cells. *Nat Rev Mol Cell Biol.* 2007; 8:729–740. doi:10.1038/nrm2233. [PubMed: 17667954]
- Chen QM. Replicative senescence and oxidant induced premature senescence: beyond the control of cell cycle checkpoints. *Ann N Y Acad Sci.* 2000; 908:111–125. [PubMed: 10911952]
- Chen Q, Ames BN. Senescence-like growth arrest induced by hydrogen peroxide in human diploid fibroblast F65 cells. *Proc Natl Acad Sci USA.* 1994; 91:4130–4134. doi:10.1073/pnas.91.10.4130. [PubMed: 8183882]
- Chen Q, Liu J, Merrett J. Apoptosis or senescence-like growth arrest: influence of cell cycle position, p53, p21 and bax in H₂O₂ response of normal human fibroblasts. *Biochem J.* 2000a; 347:543–551. doi:10.1042/0264-6021:3470543. [PubMed: 10749685]
- Chen Q, Tu V, Liu J. Measurements of hydrogen peroxide induced premature senescence: senescence-associated β -galactosidase and DNA synthesis index in human diploid fibroblasts with down-regulated p53 or Rb. *Biogerontology.* 2000b; 1:335–339. doi:10.1023/A:1026590501344. [PubMed: 11708215]
- Chen QM, Tu VC, Catania J, Burton M, Toussaint O, Dilley T. Involvement of Rb family proteins, focal adhesion proteins and de novo protein synthesis in senescent morphogenesis induced by hydrogen peroxide. *J Cell Sci.* 2000c; 113:4087–4097. [PubMed: 11058095]
- Chen Q, Prowse K, Tu V, Linskens M. Uncoupling the senescent phenotype from telomere shortening in oxidant-treated fibroblasts. *Exp Cell Res.* 2001; 265:294–303. doi:10.1006/excr.2001.5182. [PubMed: 11302695]
- Chen EI, Hewel J, Felding-Habermann B, Yates JR 3rd. Large scale protein profiling by combination of protein fractionation and multidimensional protein identification technology (MudPIT). *Mol Cell Proteomics.* 2006; 5:53–56. doi:10.1074/mcp.T500013-MCP200. [PubMed: 16272560]
- Coronella-Wood J, Terrand J, Sun H, Chen QM. c-Fos phosphorylation induced by H₂O₂ prevents proteasomal degradation of c-Fos in cardiomyocytes. *J Biol Chem.* 2004; 279:33567–33574. doi:10.1074/jbc.M404013200. [PubMed: 15136564]
- Cristofalo VJ, Lorenzini A, Allen RG, Torres C, Tresini M. Replicative senescence: a critical review. *Mech Ageing Dev.* 2004; 125:827–848. doi:10.1016/j.mad.2004.07.010. [PubMed: 15541776]
- Crowley-Weber CL, Payne CM, Gleason-Guzman M, Watts GS, Futscher B, Waltmire CN, et al. Development and molecular characterization of HCT-116 cell lines resistant to the tumor promoter and multiple stress-inducer, deoxycholate. *Carcinogenesis.* 2002; 23:2063–2080. doi:10.1093/carcin/23.12.2063. [PubMed: 12507930]
- Dalton T, Palmiter RD, Andrews GK. Transcriptional induction of the mouse metallothionein-I gene in hydrogen peroxide-treated Hepa cells involves a composite major late transcription factor/antioxidant response element and metal response promoter elements. *Nucleic Acids Res.* 1994; 22:5016–5023. doi:10.1093/nar/22.23.5016. [PubMed: 7800494]
- de Magalhaes JP, Chainiaux F, de Longueville F, Mainfroid V, Migeot V, Marcq L, et al. Gene expression and regulation in H₂O₂-induced premature senescence of human foreskin fibroblasts expressing or not telomerase. *Exp Gerontol.* 2004; 39:1379–1389. doi:10.1016/j.exger.2004.06.004. [PubMed: 15489061]
- Eng JK, McCormack AL, Yates JRI. An approach to correlate tandem mass spectral data of peptides with amino acid sequences in a protein database. *J Am Soc Mass Spectrom.* 1994; 5:976–989. doi:10.1016/1044-0305(94)80016-2. [PubMed: 24226387]
- Florens L, Washburn MP. Proteomic analysis by multidimensional protein identification technology. *Methods Mol Biol.* 2006; 328:159–175. [PubMed: 16785648]
- Gebauer F, Hentze MW. Molecular mechanisms of translational control. *Nat Rev Mol Cell Biol.* 2004; 5:827–835. doi:10.1038/nrm1488. [PubMed: 15459663]

- Hayflick L, Moorhead PS. The serial cultivation of human diploid cell strains. *Exp Cell Res.* 1961; 25:585–621. doi:10.1016/0014-4827(61)90192-6. [PubMed: 13905658]
- Hirota K, Matsui M, Iwata S, Nishiyama A, Mori K, Yodoi J. AP-1 transcriptional activity is regulated by a direct association between thioredoxin and Ref-1. *Proc Natl Acad Sci USA.* 1997; 94:3633–3638. doi:10.1073/pnas.94.8.3633. [PubMed: 9108029]
- Holcik M, Sonenberg N. Translational control in stress and apoptosis. *Nat Rev Mol Cell Biol.* 2005; 6:318–327. doi:10.1038/nrm1618. [PubMed: 15803138]
- Kang YJ. Metallothionein redox cycle and function. *Exp Biol Med.* 2006; 231:1459–1467.
- Karimpour S, Lou J, Lin LL, Rene LM, Lagunas L, Ma X, Karra S, Bradbury CM, Markovina S, Goswami PC, Spitz DR, Hirota K, Kalvakolanu DV, Yodoi J, Gius D. Thioredoxin reductase regulates AP-1 activity as well as thioredoxin nuclear localization via active cysteines in response to ionizing radiation. *Oncogene.* 2002; 21:6317–6327. doi:10.1038/sj.onc.1205749. [PubMed: 12214272]
- Kislinger T, Gramolini AO, MacLennan DH, Emili A. Multidimensional protein identification technology (MudPIT): technical overview of a profiling method optimized for the comprehensive proteomic investigation of normal and diseased heart tissue. *J Am Soc Mass Spectrom.* 2005; 16:1207–1220. doi:10.1016/j.jasms.2005.02.015. [PubMed: 15979338]
- Lee CK, Klopp RG, Weindruch R, Prolla TA. Gene expression profile of aging and its retardation by caloric restriction. *Science.* 1999; 285:1390–1393. doi:10.1126/science.285.5432.1390. [PubMed: 10464095]
- Link AJ, Eng J, Schieltz DM, Carmack E, Mize GJ, Morris DR, et al. Direct analysis of protein complexes using mass spectrometry. *Nat Biotechnol.* 1999; 17:676–682. doi:10.1038/10890. [PubMed: 10404161]
- Liu XD, Thiele DJ. Oxidative stress induced heat shock factor phosphorylation and HSF-dependent activation of yeast metallothionein gene transcription. *Genes Dev.* 1996; 10:592–603. doi:10.1101/gad.10.5.592. [PubMed: 8598289]
- Mauri P, Scarpa A, Nascimbeni AC, Benazzi L, Parmagnani E, Mafficini A, Della Peruta M, Bassi C, Miyazaki K, Sorio C. Identification of proteins released by pancreatic cancer cells by multidimensional protein identification technology: a strategy for identification of novel cancer markers. *FASEB J.* 2005; 19(9):1125–1127. [PubMed: 15985535]
- Merrick WC. Cap-dependent and cap-independent translation in eukaryotic systems. *Gene.* 2004; 332:1–11. doi:10.1016/j.gene.2004.02.051. [PubMed: 15145049]
- Mustacich D, Powis G. Thioredoxin reductase. *Biochem J.* 2000; 1:1–8. doi:10.1042/0264-6021:3460001. [PubMed: 10657232]
- Paoletti AC, Zybaylov B, Washburn MP. Principles and applications of multidimensional protein identification technology. *Expert Rev Proteomics.* 2004; 1:275–282. doi:10.1586/14789450.1.3.275. [PubMed: 15966824]
- Pascal T, Debaq-Chainiaux F, Boilan E, Ninane N, Raes M, Toussaint O. Heme oxygenase-1 and interleukin-11 are overexpressed in stress-induced premature senescence of human WI-38 fibroblasts induced by tert-butylhydro-peroxide and ethanol. *Biogerontology.* 2007; 8:409–422. doi:10.1007/s10522-007-9084-8. [PubMed: 17295091]
- Preiss T, M WH. Starting the protein synthesis machine: eukaryotic translation initiation. *Bioessays.* 2003; 25:1201–1211. doi:10.1002/bies.10362. [PubMed: 14635255]
- Purdum-Dickinson S, Lin Y, Dedek M, Johnson J, Chen Q. Induction of antioxidant and detoxification response by oxidants in cardiomyocytes: evidence from gene expression profiling and activation of the Nrf2 transcription factor. *J Mol Cell Cardiol.* 2007; 42:159–176. doi:10.1016/j.yjmcc.2006.09.012. [PubMed: 17081560]
- Sato M, Bremner I. Oxygen free radicals and metallothionein. *Free Radic Biol Med.* 1993; 14:325–337. doi:10.1016/0891-5849(93)90029-T. [PubMed: 8458590]
- Schenk H, Klein M, Erdbrugger W, Droge W, Schulze-Osthoff K. Distinct effects of thioredoxin and antioxidants on the activation of transcription factors NF-kappa B and AP-1. *Proc Natl Acad Sci USA.* 1994; 91:1672–1676. doi:10.1073/pnas.91.5.1672. [PubMed: 8127864]
- Sen CK, Packer L. Antioxidant and redox regulation of gene transcription. *FASEB J.* 1996; 10:709–720. [PubMed: 8635688]

- Shelton DN, Change E, Whittier PS, Choi D, Funk WD. Microarray analysis of replicative senescence. *Curr Biol*. 1999; 9:939–945. doi:10.1016/S0960-9822(99)80420-5. [PubMed: 10508581]
- Smith RS, Smith TJ, Blieden TM, Phipps RP. Fibroblasts as sentinel cells. Synthesis of chemokines and regulation of inflammation. *Am J Pathol*. 1997; 151:317–322. [PubMed: 9250144]
- Tabb DL, McDonald WH, Yates JR 3rd. DTASelect and contrast: tools for assembling and comparing protein identifications from shotgun proteomics. *J Proteome Res*. 2002; 1:21–26. doi:10.1021/pr015504q. [PubMed: 12643522]
- Tate DJ, Miceli MV, Newsome DA. Expression of metallothionein isoforms in human chorioretinal complex. *Curr Eye Res*. 2002; 24:12–25. doi:10.1076/ceyr.24.1.12.5426. [PubMed: 12187490]
- Washburn MP, Wolters D, Yates JR 3rd. Large-scale analysis of the yeast proteome by multidimensional protein identification technology. *Nat Biotechnol*. 2001; 19:242–247. doi:10.1038/85686. [PubMed: 11231557]
- Watts GS, Futscher BW, Isett R, Gleason-Guzman M, Kunkel MW, Salmon SE. cDNA Microarray analysis of multidrug resistance: doxorubicin selection produces multiple defects in apoptosis signaling pathways. *J Pharmacol Exp Ther*. 2001; 299:434–441. [PubMed: 11602652]
- Wei SJ, Botero A, Hirota K, Bradbury CM, Markovina S, Laszlo A, et al. Thioredoxin nuclear translocation and interaction with redox factor-1 activates the activator protein-1 transcription factor in response to ionizing radiation. *Cancer Res*. 2000; 60:6688–6695. [PubMed: 11118054]
- Wolters DA, Washburn MP, Yates JR 3rd. An automated multidimensional protein identification technology for shotgun proteomics. *Anal Chem*. 2001; 73:5683–5690. doi:10.1021/ac010617e. [PubMed: 11774908]
- Xie L, Tsapralis G, Chen QM. Proteomic identification of insulin-like growth factor binding protein-6 induced by sublethal H₂O₂ stress from human diploid fibroblasts. *Mol Cell Proteomics*. 2005; 4:1861–1873.

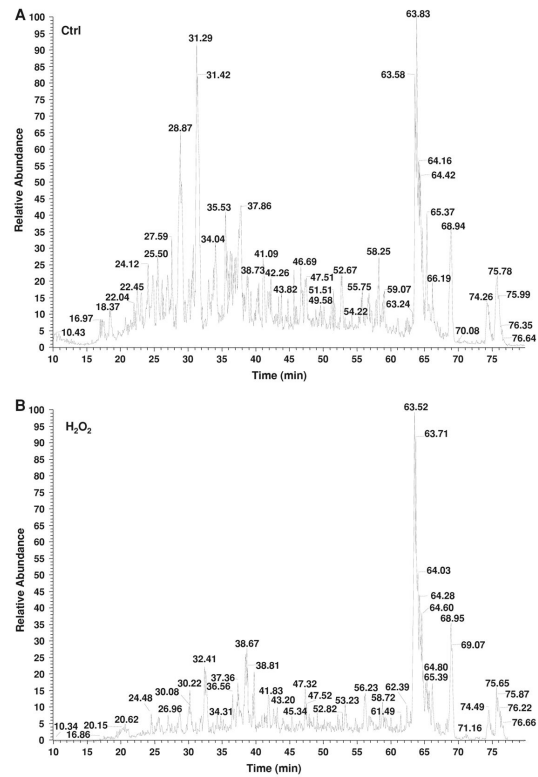


Fig. 1.

Total ion current (TIC) chromatogram of the whole cell lysate from control or H₂O₂ treated HDFs. HCA₃ fibroblasts (PDL26-40) were treated with 600 μM (~0.6 pmol/cell) of H₂O₂ for 2 h and were harvested 3 days later for dialysis, concentrating, tryptic digestion and LC-LC-MS/MS analyses. Each peak represents one parent peptide ion detected by the mass analyzer and the peak height reflects the abundance of the peptide ion

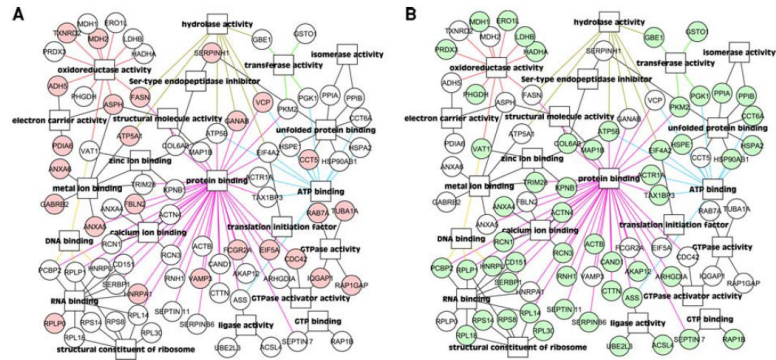


Fig. 2. Display of the proteomics data by the cytoscape network. Proteins detected only in H₂O₂ treated group (**a**, red) or control group (**b**, green) were imported into the Cytoscape 2.4.0 software for building the network. The nodes represent individual proteins and squares indicate gene ontology terms. The colors of the edges enhance the view of corresponding gene ontology groups in the network of microarray data

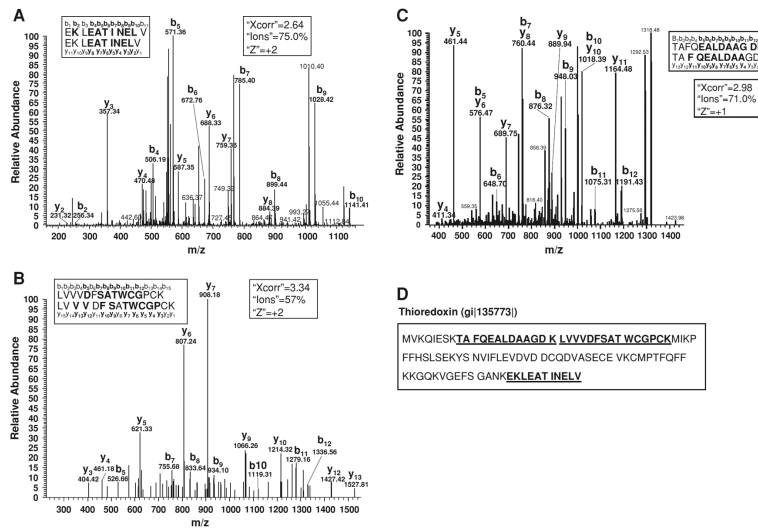


Fig. 3. MS/MS Spectra of Thioredoxin Peptides Detected from H₂O₂ treated HDFs. The bolded letters indicate the detected b and y ions matching with the predicted ions in the protein sequence database (a–c). SEQUEST Flicka protein information shows the fragments detected relative to the complete sequence of thioredoxin protein (d)

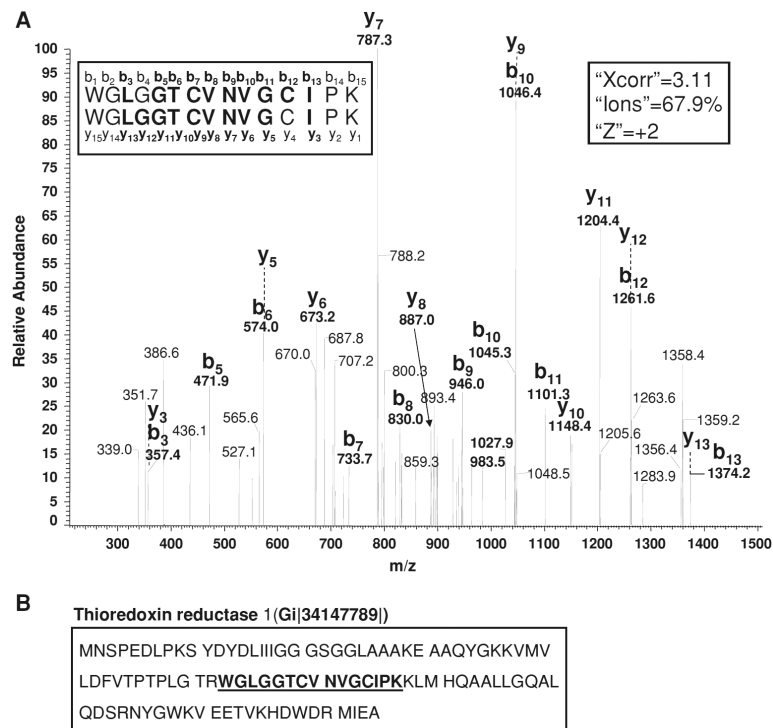


Fig. 4. MS/MS Spectrum of Thioredoxin Reductase 1 Peptide Detected from H₂O₂-treated HDFs. The bolded letters indicate the detected b and y ions matching the predicted ion mass in the database (a). SEQUEST Flicka protein information shows the fragment detected relative to the complete sequence of thioredoxin reductase 1 protein (b)

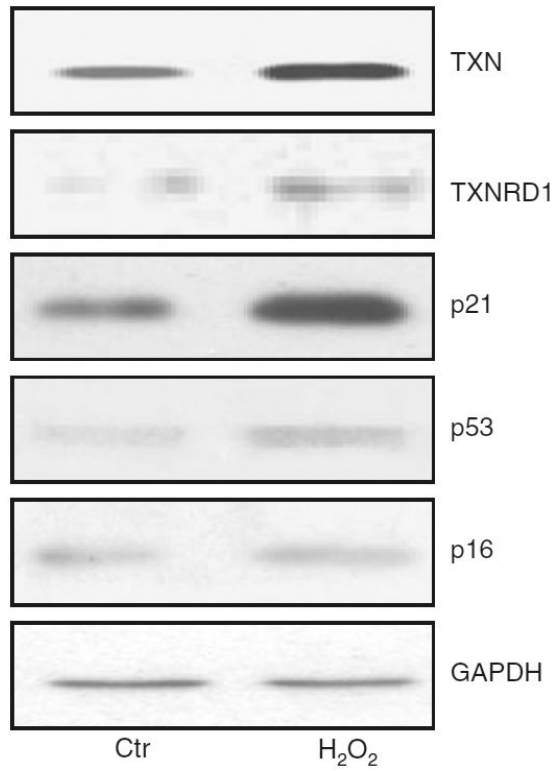


Fig. 5. Increased TXN and TXNRD1 Protein Levels in the H₂O₂ Treated Cells. HDFs were treated with 600 μ M H₂O₂ for 2 h. Cells were harvested 3 days after for SDS-PAGE and Western blot analyses to detect TXN, TXNRD1, p53, p21 and p16. GAPDH was used as a loading control to show equal amount of proteins between different groups of samples

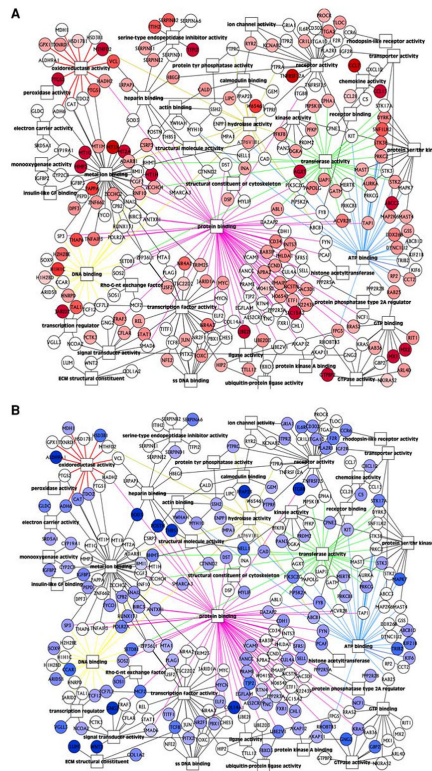


Fig. 6. The network of genes increased or decreased in H₂O₂ treated cells. HDFs were treated with 600 μM H₂O₂ for 2 h. Microarray analyses were performed using RNA collected 72 h after H₂O₂ treatment. The nodes represent genes increasing (a, red) or decreasing (b, blue) in H₂O₂ treated cells. The color shades of nodes reflect the degree of changes, with darker color indicating more increase (red) or decrease (blue) than the lighter shade of color. The squares represent gene ontology terms. The colors of the edges enhance the view of corresponding gene ontology groups in the network of proteomic data

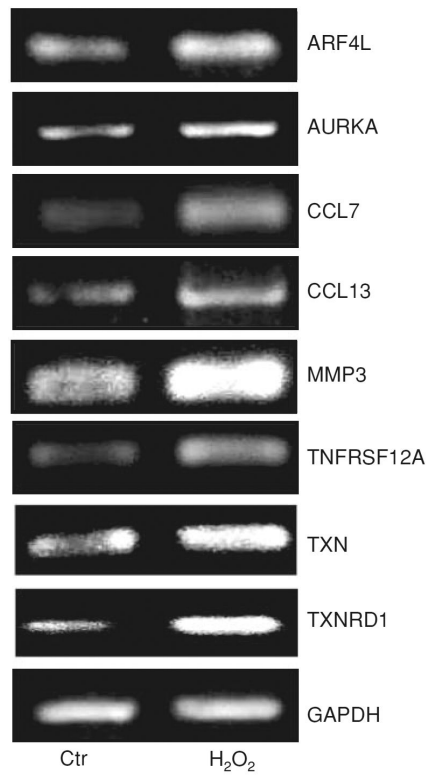


Fig. 7.

Increased mRNA levels of the genes detected in H₂O₂ treated HDFs. HDFs were treated with 600 μ M H₂O₂ for 2 h. Cells were placed in fresh DMEM containing 10% FBS for 3 days before harvesting. Total RNA (2 μ g) was used for reverse transcription (RT) and 3 μ l of the 35 μ l RT reaction mixture was used for each PCR to amplify ARF4L (ADP-ribosylation factor 4-like), AURKA (Serine/threonine kinase 15), CCL7 (Small inducible cytokine A7), CCL13 (Small inducible cytokine subfamily A13), MMP3 (Matrix metalloproteinase 3), TXN (Thioredoxin), TXNRD1 (Thioredoxin reductase 1), TNFRSF12A (Tumor necrosis factor receptor superfamily, member 12A). GAPDH was amplified to show equal amount of RNAs between each sample

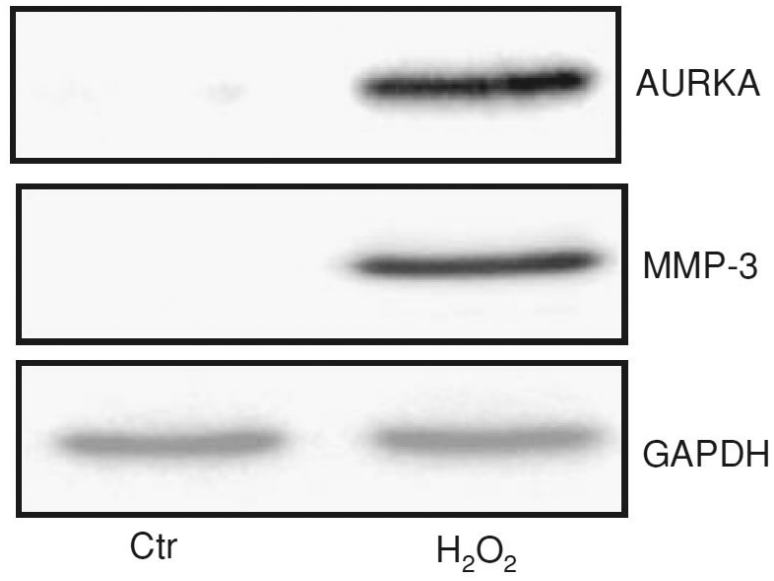


Fig. 8. Increased protein levels of AURKA and MMP-3. HDFs were treated with 600 μ M H₂O₂ for 2 h. Cell lysates were collected 72 h after H₂O₂ treatment to perform Western blot analyses to detect MMP3 and AURKA. GAPDH was used as a loading control to show equal amount of proteins between samples

Table 1

Sequence, expected size of product and annealing temperature of PCR primers

Symbol	Gene	PCR Primer sequences	Fragment (bp)	TempA (°C)
ARF4L	ADP-ribosylation factor 4-like	5'ggggaaccacttgactgaga 5'tcttcctgggttgaagcct	171	62
AURKA	Serine/threonine kinase 15	5'tgaggagggaactggcatcaa 5'gaccacccaaaatctgcaat	208	62
CCL7	Small inducible cytokine A7	5'atgaaagcctctgcagcact 5'ggacagtggctactggtggt	179	64
CCL13	Small inducible cytokine A13	5'atctccttcagaggctgaa 5'cttcagggtgtgagctttcc	165	62
MMP3	Matrix metalloproteinase 3	5'gcagtttgctcagcctatcc 5'gagtgtcggagtccagcttc	214	62
TXNRD1	Thioredoxin reductase 1	5'attgccactggtgaaagacc 5'accatttttggccatgt	185	55
TXN	Thioredoxin	5'ctgcttttcaggaagccttg 5'tgttggcatgcattgactt	203	53
GAPDH	Glyceraldehyde-3-phosphate dehydrogenase	5'cgtcttcacatggaga 5'cgccatcaccccacagttt	238	62

Table 2

Proteins found in control (Italic) or H₂O₂-treated HDFs

(1) Gene symbol	(2) Gi #	(3) Common name	(4) Xcorr (± SD)	(5) Charge (Pep#), sequence & coverage
Oxidoreductase/antioxidants/detoxification				
<i>ERO1L</i> %	14250470	<i>ERO1-like</i>	2.74	<i>d</i> ₊₂ (1), <i>e</i> LGAVDESLSEETQK, <i>f</i> 3.0%
<i>GSTO1</i> %	4758484	<i>Glutathione-S-transferase omega 1</i>	2.59	<i>d</i> ₊₂ (1), <i>e</i> EDPTVSALLTSEK, <i>f</i> 4.5%
<i>HADHA</i>	20127408	<i>Hydroxyacyl dehydrogenase, subunit A</i>	2.79	<i>d</i> ₊₂ (1), <i>e</i> TGIEQGS DAGYLCESQK, <i>f</i> 2.2%
<i>LDHB</i> %	4557032	<i>Lactate dehydrogenase B</i>	3.41 ± 0.72	<i>d</i> ₊₂ (2), <i>f</i> 9.3%
<i>MDH1</i>	7431153	<i>Malate dehydrogenase, cytosolic</i>	4.38	<i>d</i> ₊₂ (1), <i>e</i> VIVVGNPANTNCLTASK, <i>f</i> 5.1%
<i>PRDX3</i>	23308577	<i>Peroxiredoxin 3 isoform a</i>	3.32	<i>d</i> ₊₂ (1), <i>e</i> AGTGV DNV DLEAATR, <i>f</i> 2.8%
<i>PHGDH</i>	5802974	<i>Phosphoglycerate dehydrogenase</i>	4.09	<i>d</i> ₊₂ (1), <i>e</i> DYGV LLEGSGLALR, <i>f</i> 5.5%
<i>ADH5</i>	11496891	<i>Alcohol dehydrogenase III5 chi subunit</i>	4.02 ± 1.24	<i>d</i> ₊₂ (2), <i>f</i> 9.6%
<i>ASPH</i> %	14589860	<i>Aspartate beta-hydroxylase isoform c</i>	4.04	<i>d</i> ₊₂ (1), <i>e</i> LG IYDADGDGDFD VDDAK, <i>f</i> 5.8%
<i>MDH2</i> %	21735621	<i>Mitochondrial malate dehydrogenase</i>	3.58 ± 1.24	<i>d</i> ₊₂ (4), <i>f</i> 18.0%
<i>PDIA6</i> %	5031973	<i>Protein disulfide isomerase A6</i>	3.49 ± 0.94	<i>d</i> ₊₂ (2), <i>f</i> 6.5%
<i>TXN</i> %	135773	<i>Thioredoxin</i>	<i>a</i> 2.98, 2.99 ± 0.49	<i>d</i> ₊₁ (1), <i>d</i> ₊₂ (2), <i>f</i> 37.1%
<i>TXNRD1</i>	34147789	<i>Thioredoxin reductase 1</i>	3.11	<i>d</i> ₊₂ (1), <i>e</i> WGLGGTCVNVGCIPK, <i>f</i> 2.9%
Metabolic enzymes				
<i>ALDOA</i> %	4557305	<i>Aldolase A</i>	4.10 ± 0.14	<i>d</i> ₊₂ (2), <i>f</i> 10.2%
<i>ASS</i> %	16950633	<i>Argininosuccinate synthetase</i>	2.53	<i>d</i> ₊₂ (1), <i>e</i> FELSCYSLAPQIK, <i>f</i> 3.2%
<i>GBE1</i>	15082371	<i>Glucan, branching enzyme 1</i>	3.12	<i>d</i> ₊₂ (1), <i>e</i> VALILQNV DLPN, <i>f</i> 1.7%
<i>GOT2</i>	12653507	<i>Glutamic-oxaloacetic transaminase 2</i>	4.11	<i>d</i> ₊₂ (1), <i>e</i> FVTVQTISGTGALR, <i>f</i> 3.3%
<i>PPIA</i>	10863927	<i>Peptidylprolyl isomerase A</i>	3.10 ± 0.36	<i>d</i> ₊₂ (2), <i>f</i> 12.1%
<i>PPIB</i>	118090	<i>Peptidyl-prolyl cis-trans isomerase B</i>	<i>a</i> 2.14, 3.53	<i>d</i> ₊₁ (1), <i>d</i> ₊₂ (1), <i>f</i> 10.1%
<i>PGK1</i> %	129902	<i>Phosphoglycerate kinase 1</i>	4.78 ± 0.19	<i>d</i> ₊₂ (2), <i>f</i> 8.1%
<i>PKM2</i> %	33286420	<i>Pyruvate kinase 3 isoform 2</i>	3.87 ± 1.01	<i>d</i> ₊₂ (9), <i>f</i> 22.6%
<i>PSAP</i> %	30235	<i>Cerebroside sulfate activator</i>	3.80	<i>d</i> ₊₂ (1), <i>e</i> EIVDSYLPVILDIIK, <i>f</i> 22.4%
<i>FASN</i>	1345959	<i>Fatty acid synthase</i>	3.91 ± 1.36	<i>d</i> ₊₂ (2), <i>f</i> 1.4%
<i>GBA</i> %	183012	<i>Glucocerebrosidase</i>	3.46	<i>d</i> ₊₂ (1), <i>e</i> PVSL LASPWTSP T WLK, <i>f</i> 3.0%
<i>GANAB</i> %	2274968	<i>Glucosidase II</i>	2.60	<i>d</i> ₊₂ (1), <i>e</i> VPDVLVADPPIAR, <i>f</i> 1.4%
<i>ECHS1</i>	433413	<i>Mitochondrial short-chain enoyl-CoA hydratase</i>	2.98	<i>d</i> ₊₂ (1), <i>e</i> ALNALCDGLIDELNQALK, <i>f</i> 6.2%
<i>NANS</i> %	12056473	<i>N-acetylneuraminic acid phosphate synthase</i>	4.19 ± 0.91	<i>d</i> ₊₂ (4), <i>f</i> 2.8%
Receptor activity				
<i>M6PRBP1</i> %	20127486	<i>Mannose-6-phosphate receptor binding protein 1</i>	3.41	<i>d</i> ₊₂ (1), <i>e</i> IATSLDGF DVASVQQQR, <i>f</i> 3.9%
<i>TAX1BP3</i>	11993943	<i>Tax interaction protein 1</i>	3.99	<i>d</i> ₊₂ (1), <i>e</i> VSEGGPAE IAGLQIGDK, <i>f</i> 13.7%
<i>GABRB2</i> %	12548785	<i>GABA A receptor, beta 2 isoform 1</i>	2.64	<i>d</i> ₊₂ (1), <i>e</i> LDV NKIFYKDIK, <i>f</i> 2.3%
Transport activity				
<i>ATP1B3</i>	4502281	<i>ATPase, Na⁺/K⁺ + transporting, beta 3</i>	2.67	<i>d</i> ₊₂ (1), <i>e</i> LFIYNPTTGEFLGR, <i>f</i> 5.0%

(1) Gene symbol	(2) Gi #	(3) Common name	(4) Xcorr (\pm SD)	(5) Charge (Pep#), sequence & coverage
<i>ATP5B</i>	32189394	<i>ATP synthase, H + transporting, mitochondrial F1 complex, beta</i>	3.67	$d_{+2}(1)$, c AIAELGIYPAVDPLDSTSR, f 6.1%
<i>KPNB1</i>	19923142	<i>Karyopherin beta 1</i>	2.81 ± 0.12	$d_{+2}(2)$, f 3.5%
Signaling molecules				
<i>ANXA4</i>	34365437	<i>Annexin A4</i>	3.47	$d_{+2}(1)$, c SETSGSFEDALLAIVK, f 14.3%
<i>GNG12</i> [%]	12229817	<i>Guanine nucleotide-binding protein G(I)/G(S)/G(O) gamma-12 subunit</i>	3.53	$d_{+2}(1)$, c SDPLLIGIPTSENPFK, f 22.2%
<i>RAP1B</i>	7661678	<i>RAS-related protein RAP1B</i>	3.76	$d_{+2}(1)$, c INVNEIFYDLVR, f 1.6%
<i>STIP1</i>	5803181	<i>Stress-induced-phosphoprotein 1</i>	3.43	$d_{+2}(1)$, c ALSVGNIDDALQCYSEAIK, f 3.5%
ANP32B [%]	5454088	Acidic nuclear phosphoprotein 32 family, member B	3.51	$d_{+2}(1)$, c SLDLFNCEVTNLNDYR, f 8.2%
ANXA5 [%]	3212603	Annexin V With Proline Substitution By Thioproline	a 2.05 \pm 0.09; b 3.82 \pm 0.76	$d_{+1}(3)$, $d_{+2}(4)$, f 22.5%
CDC42	16357472	cell division cycle 42 isoform 2	2.61	$d_{+2}(1)$, c TPFLLVGTQIDLR, f 6.8%
CAP1 [%]	33357226	C-Terminal Cap1-Adenylyl Cyclase Associated Protein Chain A	5.03	$d_{+2}(1)$, c VENQENVSNLVIEDTELK, f 11.5%
EIF3S5 [%]	30584931	Eukaryotic translation initiation factor 3, subunit 5 epsilon	3.83	$d_{+2}(1)$, c VIGLSSDLQQVVGASAR, f 4.9%
IQGAP1	40674640	IQGAP1 protein	4.03	$d_{+2}(1)$, c ILAIGLINEALDEGDAQK, f 1.9%
MVP	5851638	Major vault protein	3.07 ± 0.29	$d_{+2}(2)$, f 20.1%
TBX20 [%]	13431875	Putative S100 calcium-binding protein	3.86	$d_{+2}(1)$, c TEFLSFMNTELAFTK, f 15.4%
GDI2	4960030	Rab GDP dissociation inhibitor beta	3.67	$d_{+2}(1)$, c TDDYLDQPCYETINR, f 4.2%
RAP1GAP [%]	34327960	RAP1 GTPase activating protein	2.54	$d_{+2}(1)$, c GSAIGIGTVEEVVVR, f 2.2%
SET	1711383	SET protein	3.70	$d_{+2}(1)$, c IDFYFDENPYFENK, f 5.1%
GNB1	3387975	Signal transducing proteins GS/GI beta-subunit	3.09	$d_{+2}(1)$, c LLLAGYDDFNCNVWDALK, f 14.2%
RAB7	1174149	Small GTP binding protein Rab7	3.20	$d_{+2}(1)$, c GADCCVLVFDVTAPNTFK, f 8.7%
Peptidases and inhibitors				
<i>PPGB</i> [%]	12653639	<i>Protective protein for beta-galactosidase</i>	3.22	$d_{+2}(1)$, c DLECVTNLQEVAR, f 2.7%
<i>PSMA7</i> [%]	4506189	<i>Proteasome subunit, alpha type, 7</i>	3.90 ± 0.07	$d_{+2}(2)$, f 16.3%
<i>SERPINB6</i>	20141722	<i>Serpin peptidase inhibitor, clade B, member 6</i>	2.82	$d_{+2}(1)$, c IAELLSPGSVDPLTR, f 4.0%
CTSB [%]	115711	Cathepsin B precursor	3.63	$d_{+2}(1)$, c NGPVEGAFSVYSDFLLYK, f 5.3%
PSMA2	4506181	Proteasome alpha 2 subunit	3.72	$d_{+2}(1)$, c AAVPSGASTGIYEALR, f 4.1%
Structural				
<i>ACTN4</i>	12025678	<i>Actinin, alpha 4</i>	3.64 ± 0.93	$d_{+2}(3)$, f 4.4%
<i>ACTRIA</i>	5031569	<i>ARP1 actin-related protein 1 homolog A, centractin alpha</i>	4.02 ± 0.97	$d_{+2}(2)$, f 8.8%
<i>Arp11</i>	12583652	<i>Actin-related protein Arp11</i>	3.39	$d_{+2}(1)$, c DITYFIQQLLR, f 5.2%
<i>ACTB</i>	16359158	<i>Beta actin</i>	3.65 \pm 1.11, c 4.21	$d_{+2}(4)$, $d_{+3}(1)$, f 16.0%
<i>CALD1</i> [%]	4826657	<i>Caldesmon 1 isoform 3</i>	3.08	$d_{+2}(1)$, c EFDPTTIDASLSLPSR, f 3.3%
<i>COL6A1</i> [%]	1360676	<i>Collagen alpha 1(VI) chain</i>	4.93	$d_{+2}(1)$, c LLLFSDGNSQGATPAAIEK, f 1.8%
<i>COL6A2</i>	105706	<i>Collagen alpha 2(VI) chain</i>	4.13	$d_{+2}(1)$, c NLEWIAGGTWTPSALK, f 6.7%

(1) Gene symbol	(2) Gi #	(3) Common name	(4) Xcorr (\pm SD)	(5) Charge (Pep#), sequence & coverage
<i>COL6A3</i>	17149807	Collagen alpha 3 (VI) isoform 3	3.29 \pm 0.96	$d_{+2}(2)$, $f_{1.0}\%$
<i>FSCN1</i> %	13623415	Fascin 1	3.14	$d_{+2}(1)$, e ASAETVDPASLWEY, $f_{2.8}\%$
<i>FERIL3</i>	10834587	Fer-1 like protein 3	4.06	$d_{+2}(1)$, e NLVDPFVVEVSFAGK, $f_{0.7}\%$
<i>GSN</i> %	17028367	Similar to gelsolin	3.28 \pm 0.02	$d_{+2}(2)$, $f_{10.9}\%$
<i>RPL18</i> %	4506607	Ribosomal protein L18	2.87	$d_{+2}(1)$, e ILTFDQLALDSPK, $f_{6.9}\%$
<i>RPS8</i> %	4506743	Ribosomal protein S8	3.16	$d_{+2}(1)$, e NCIVLIDSTPYR, $f_{5.8}\%$
<i>TUBA1A</i> %	30584771	Tubulin alpha 1	3.87 \pm 0.88; c 3.76	$d_{+2}(5)$, $d_{+3}(1)$, $f_{18.0}\%$
TPM2 %	6573280	Beta tropomyosin	3.01	$d_{+2}(1)$, e LVILEGELER, $f_{3.5}\%$
CAPZB %	13124696	F-actin capping protein beta subunit	2.93	$d_{+2}(1)$, e GCWDSIHVVEVQEK, $f_{5.1}\%$
LAMP1	39645231	LAMP1 protein	5.20	$d_{+2}(1)$, e FFLQGIQLNTILPDAR, $f_{6.5}\%$
MSN	14625824	Moesin/anaplastic lymphoma kinase fusion protein	4.74	$d_{+2}(1)$, e FYPEDVSEELIQDITQR, $f_{3.2}\%$
TUBB	56757569	Tubulin beta-1 chain	4.48 \pm 0.53	$d_{+2}(2)$, $f_{7.2}\%$
Protein binding				
<i>AKAP12</i>	21493022	A-kinase anchor protein 12 isoform 1	4.50	$d_{+2}(1)$, e LVQNIQTAVDQFVR, $f_{0.8}\%$
<i>HSPE1</i>	4008131	Chaperonin 10	4.06	$d_{+2}(1)$, e VLQATVVAVGSGSK, $f_{14.1}\%$
<i>CCT6A</i>	4502643	Chaperonin containing TCP1 subunit 6A	2.85	$d_{+2}(1)$, e AQLGVQAFADALLIIPK, $f_{3.2}\%$
<i>CTTN</i> %	20357552	Cortactin isoform a	2.65	$d_{+2}(1)$, e YGLFPANYVELR, $f_{2.2}\%$
<i>HSP90AB1</i> %	20149594	Heat shock protein 90-beta	4.08 + -0.62	$d_{+2}(3)$, $f_{5.3}\%$
<i>HSPA2</i> %	13676857	Heat shock 70 kDa protein 2	3.40 \pm 0.82	$d_{+2}(2)$, $f_{6.1}\%$
<i>MAP1B</i> %	14165456	Microtubule-associated protein 1B isoform 2	4.07	$d_{+2}(1)$, e NLISPDLVVFLNVPENLK, $f_{0.8}\%$
<i>RCN1</i>	4506455	Reticulocalbin 1 precursor	3.42 \pm 0.19	$d_{+2}(2)$, $f_{8.5}\%$
<i>RCN3</i> %	28626510	Reticulocalbin 3, EF-hand calcium binding domain	4.81	$d_{+2}(1)$, e DIVIAETLEDLDR, $f_{4.0}\%$
<i>RNHI</i> %	35844	Ribonuclease/angiogenin inhibitor	3.38 \pm 0.69	$d_{+2}(3)$, $f_{10.6}\%$
<i>CAND1</i> %	21361794	TIP120 protein	3.93	$d_{+2}(1)$, e ISGSILNELIGLVR, $f_{2.5}\%$
CCT5	24307939	Chaperonin containing TCP1, subunit 5	3.25	$d_{+2}(1)$, e WVGPEIELIAIATGGR, $f_{3.2}\%$
AHNAK %	627367	Desmoyokin	3.00 \pm 0.26	$d_{+2}(8)$, $f_{4.2}\%$
FCGR2A %	34419635	Heat shock 70 kDa protein 6	4.02	$d_{+2}(1)$, e IINEPTAAAIAYGLDR, $f_{2.5}\%$
SERPINH1 %	8574449	Rheumatoid arthritis-related antigen RA-A47	3.71 \pm 0.07	$d_{+2}(2)$, $f_{18.6}\%$
VCP %	6005942	Valosin-containing protein	3.07 \pm 0.23	$d_{+2}(3)$, $f_{7.5}\%$
VAMP3	13543574	Vesicle-associated membrane protein 3	3.48	$d_{+2}(1)$, e ADALQAGASQFETSAAK, $f_{17.0}\%$
DNA/RNA/nucleotide binding				
<i>EIF4A2</i>	16198386	Eukaryotic translation initiation factor 4A, isoform 2	2.77	$d_{+2}(1)$, e GYDVIAQAQSGTGK, $f_{3.4}\%$
<i>HNRPU</i>	14141161	Heterogeneous nuclear ribonucleoprotein U isoform b	2.12	$d_{+1}(1)$, e VSELKEELK, $f_{1.1}\%$
<i>HNRPD</i>	870747	Heterogeneous nuclear ribonucleoprotein D	2.66	$d_{+2}(1)$, e IFVGGLSPDTPEEK, $f_{4.9}\%$
<i>SERBP1</i> %	7661626	PAI-1 mRNA-binding protein	3.51	$d_{+2}(1)$, e FDQLFDESDFEVLK, $f_{4.0}\%$

(1) Gene symbol	(2) Gi #	(3) Common name	(4) Xcorr (\pm SD)	(5) Charge (Pep#), sequence & coverage
<i>PCBP2</i>	14141166	<i>Poly(rC)-binding protein 2 isoform b</i>	2.75	$d_{+2}(1)$, c AITLAGIPQSIIECVK, f 4.4%
<i>RPL14</i> [%]	7513316	<i>Ribosomal protein L14</i>	4.45	$d_{+2}(1)$, c LVAIVDVIDQNR, f 5.4%
<i>CD151</i>	4506671	<i>Ribosomal protein P2</i>	3.40 \pm 0.28	$d_{+2}(2)$, f 27.8%
<i>RPS14</i>	5032051	<i>Ribosomal protein S14</i>	3.14	$d_{+2}(1)$, c IEDVTPIPSDSTR, f 8.6%
<i>septin 11</i> [%]	33873799	<i>Septin11</i>	3.44	$d_{+2}(1)$, c LTIVDTVGFQDQINK, f 3.1%
<i>TRIM28</i>	5032179	<i>Tripartite motif-containing 28 protein</i>	2.57	$d_{+2}(1)$, c LDLTLTADSQPPVFK, f 1.8%
EIF5A [%]	33383425	Eukaryotic initiation factor 5A isoform I variant A	4.29	$d_{+2}(1)$, c NDFQLIGIQDGYLSLLQDS GEVR, f 12.5%
HNRPA1	133252	Heterogeneous nuclear ribonucleoprotein A1	3.19	$d_{+2}(1)$, c LFIGGLSFETTESLR, f 8.2%
RPL6 [%]	16753227	Ribosomal protein L6	3.29	$d_{+2}(1)$, c ASITPGTILILTGR, f 5.2%
RPLP0 [%]	4432757	Ribosomal protein P0	4.30	$d_{+2}(1)$, c VLALSIVETDVTPLAEK, f 18.3%
Miscellaneous				
<i>BLOCK 23</i> [%]	20853684	<i>BLOCK 23</i>	3.28 \pm 0.75	$d_{+2}(2)$, f 7.9%
<i>NAPIL2</i> [%]	30584347	<i>Homo sapiens nucleosome assembly protein 1-like 2</i>	3.10	$d_{+2}(1)$, c LDGLVETPTGYIESLPR, f 4.3%
<i>VAT1</i> [%]	18379349	<i>Vesicle amine transport protein 1(BRCA1)</i>	3.38	$d_{+2}(1)$, c TVENVTVFGTASASK, f 3.8%
ATP5A1 [%]	34782901	ATP5A1 protein	3.54	$d_{+2}(1)$, c TGAIVDVPVGEELLGR, f 3.6%
FBLN2	4884120	Hypothetical protein	5.36	$d_{+2}(1)$, c IGPAPAFTGDTIALNIIK, f 3.1%
RAP1GAP [%]	34327960	RAP1 GTPase activating protein	2.54	$d_{+2}(1)$, c GSAIGTVEEVVVR, f 2.2%
TMC5 [%]	31377679	Transmembrane channel-like 5	a 1.90	$d_{+1}(1)$, c NQPRTMEEKR, f 1.5%

Cell lysates were prepared as described in the Methods for MudPIT and MS/MS analyses. The proteins unique to Control group (in italic) or H₂O₂ treated group are listed here. All proteins meet the selection criteria of Xcorr = 1.8 for +1 ions, Xcorr = 2.5 for +2 ions and Xcorr = 3.5 for +3 ions. The value of Ions exceeds 50% in all cases by Turbo SEQUEST analyses. The column in the table represents (1) Gene symbol. The sign[%] marks the protein whose corresponding cDNAs was not on the list of genes in Human 5 k cDNA microarray chip; (2) Gi number; (3) common name of the protein; (4) Xcorr values for +2 peptide ions, means \pm standard deviations, unless specifically labeled. The letter *a* indicates Xcorr values for +1 peptide ions, while the letter *c* indicates Xcorr values for +3 peptide ions; (5) The letter *d* indicates the charge of detected peptide ions with the number of detected peptide ions shown in a parenthesis. The letter *e* denotes the peptide sequence if only one peptide ion was detected for the protein. The letter *f* represents the percentage of coverage of detected peptides over total protein sequences. A number of proteins can be placed under multiple functional categories. For clarification, these proteins are placed under the category of their most commonly recognized function

Table 3cDNA Microarray detection of genes changing expression in HDFs with H₂O₂ treatment

(1) Gene symbol	(2) Accession	(3) Gene name	(4) Unigene	(5) Fold of changes
Oxidoreductase/antioxidants				
GCLM	JC2474	Glutamate-cysteine ligase, modifier subunit	Hs.315562	1.89 ± 0.01
GPX1	AA485362	Glutathione peroxidase 1	Hs.76686	1.74 ± 0.21
GSS	AA463458	Glutathione synthetase	Hs.82327	1.68 ± 0.14
HADH2	AA458661	Hydroxyacyl-Coenzyme A dehydrogenase, type II	Hs.171280	1.99 ± 0.33
LOX	AA453085	Lysyl oxidase	Hs.102267	3.47 ± 2.08
MT1A	H72722	Metallothionein 1A (functional)	Hs.513626	3.74 ± 2.56
MT1E	AA872383	Metallothionein 1E	Hs.534330	3.24 ± 1.66
MT1G	H53340	Metallothionein 1G	Hs.433391	3.90 ± 2.45
MT1H	H77766	Metallothionein 1H	Hs.438462	3.26 ± 1.59
MT1M	AA570216	Metallothionein 1M	Hs.647370	2.89 ± 1.38
MT1X	N80129	Metallothionein 1X	Hs.374950	3.54 ± 2.39
MT2A	AI024402	Metallothionein 2A	Hs.647371	3.47 ± 2.01
MTHFD2	AA480995	Methylenetetrahydrofolate dehydrogenase 2	Hs.469030	3.47 ± 2.72
NAGLU	W07099	N-acetylglucosaminidase, alpha	Hs.50727	1.55 ± 0.06
PTGS1	AA454668	Prostaglandin-endoperoxide synthase 1	Hs.201978	2.50 ± 0.74
PTGS2	AA644211	Prostaglandin-endoperoxide synthase 2	Hs.196384	4.91 ± 4.39
TXNRD1	AA453335	Thioredoxin reductase 1	Hs.654922	2.76 ± 1.88
<i>ADH6</i>	<i>H68509</i>	<i>Alcohol dehydrogenase 6 (class V)</i>	<i>Hs.586161</i>	<i>-2.32 ± 1.09</i>
<i>ALDH9A1</i>	<i>R25818</i>	<i>Aldehyde dehydrogenase 9 family, member A1</i>	<i>Hs.2533</i>	<i>-4.85 ± 5.11</i>
<i>BBS9</i>	<i>T58298</i>	<i>Bardet-Biedl syndrome 9</i>	<i>Hs.372360</i>	<i>-1.78 ± 0.23</i>
<i>CAT</i>	<i>N77183</i>	<i>Catalase</i>	<i>Hs.502302</i>	<i>-2.18 ± 0.59</i>
<i>CYP2A6</i>	<i>T73031</i>	<i>Cytochrome P450, subfamily IIA, polypeptide 6</i>	<i>Hs.439056</i>	<i>-2.36 ± 1.15</i>
<i>CYP2C8</i>	<i>N53136</i>	<i>Cytochrome P450, subfamily IIC, polypeptide 8</i>	<i>Hs.282871</i>	<i>-1.56 ± 0.05</i>
<i>FMO5</i>	<i>H52001</i>	<i>Flavin containing monooxygenase 5</i>	<i>Hs.303476</i>	<i>-1.86 ± 0.40</i>
<i>GLDC</i>	<i>N78083</i>	<i>Glycine dehydrogenase</i>	<i>Hs.573072</i>	<i>-2.43 ± 0.30</i>
<i>HSD3B1</i>	<i>R68803</i>	<i>Hydroxy-delta-5-steroid dehydrogenase, 3 beta- and steroid delta-isomerase 1</i>	<i>Hs.364941</i>	<i>-2.75 ± 1.15</i>
<i>MDH1</i>	<i>H83233</i>	<i>Malate dehydrogenase 1, NAD (soluble)</i>	<i>Hs.526521</i>	<i>-1.81 ± 0.26</i>
<i>NELL1</i>	<i>W16715</i>	<i>NEL-like 1</i>	<i>Hs.502145</i>	<i>-2.66 ± 0.67</i>
<i>SOD3</i>	<i>AA725564</i>	<i>Superoxide dismutase 3, extracellular</i>	<i>Hs.2420</i>	<i>-4.19 ± 0.19</i>
<i>SRD5A1</i>	<i>R36874</i>	<i>Steroid-5-alpha-reductase, alpha polypeptide 1</i>	<i>Hs.552</i>	<i>-1.89 ± 0.45</i>
<i>TDO2</i>	<i>T72422</i>	<i>Tryptophan 2,3-dioxygenase</i>	<i>Hs.183671</i>	<i>-2.04 ± 0.36</i>
Metabolic enzymes				
AGXT	N57872	Alanine-glyoxylate aminotransferase	Hs.144567	12.62 ± 13.06
DERA	N74602	2-deoxyribose-5-phosphate aldolase homolog	Hs.39429	1.73 ± 0.16
FPGS	R44864	Folylpolyglutamate synthase	Hs.335084	1.81 ± 0.18
INPPL1	AA279072	Inositol polyphosphate phosphatase-like 1	Hs.523875	2.35 ± 0.42
UNG2	AA425900	Uracil-DNA glycosylase 2	Hs.3041	1.57 ± 0.06

(1) Gene symbol	(2) Accession	(3) Gene name	(4) Unigene	(5) Fold of changes
<i>CAD</i>	<i>R84263</i>	<i>Carbamoyl-phosphate synthetase 2, aspartate transcarbamylase, and dihydroorotase</i>	<i>Hs.377010</i>	-2.03 ± 0.36
<i>NM_024843</i>	<i>N75713</i>	<i>Cytochrome b reductase 1</i>	<i>Hs.221941</i>	-2.61 ± 0.24
<i>GYS2</i>	<i>N72934</i>	<i>Glycogen synthase 2</i>	<i>Hs.82614</i>	-1.62 ± 0.04
<i>SHMT1</i>	<i>R53294</i>	<i>Serine hydroxymethyltransferase 1</i>	<i>Hs.513987</i>	-2.07 ± 0.81
<i>UGCGL1</i>	<i>R98442</i>	<i>UDP-glucose ceramide glucosyltransferase-like 1</i>	<i>Hs.34180</i>	-1.73 ± 0.28
Transferases				
<i>DNMT1</i>	<i>H09055</i>	<i>DNA-methyltransferase 1</i>	<i>Hs.202672</i>	2.43 ± 0.38
<i>GATM</i>	<i>R61229</i>	<i>Glycine amidinotransferase</i>	<i>Hs.75335</i>	1.68 ± 0.02
<i>GBE1</i>	<i>A46075</i>	<i>Glucan (1,4-alpha-), branching enzyme 1</i>	<i>Hs.436062</i>	1.91 ± 0.44
<i>GALNT2</i>	<i>R00595</i>	<i>UDP-N-acetyl-alpha-D-galactosamine: N-acetylgalactosaminyltransferase 2</i>	<i>Hs.567272</i>	1.89 ± 0.41
<i>UAP1</i>	<i>H78134</i>	<i>UDP-N-acetylglucosamine pyrophosphorylase 1</i>	<i>Hs.492859</i>	2.62 ± 1.30
<i>ZCCHC4</i>	<i>R91215</i>	<i>Zinc finger, CCHC domain containing 4</i>	<i>Hs.278945</i>	1.75 ± 0.25
<i>BHMT</i>	<i>T58958</i>	<i>Betaine-homocysteine methyltransferase</i>	<i>Hs.80756</i>	-2.41 ± 0.75
<i>SETDB1</i>	<i>R12070</i>	<i>SET domain, bifurcated 1</i>	<i>Hs.516278</i>	-2.61 ± 1.55
<i>ART4</i>	<i>N70349</i>	<i>Translin</i>	<i>Hs.13776</i>	-1.60 ± 0.07
Phosphatases				
<i>DUSP5</i>	<i>W65461</i>	<i>Dual specificity phosphatase 5</i>	<i>Hs.2128</i>	2.53 ± 1.38
<i>PPAP2B</i>	<i>T72119</i>	<i>Phosphatidic acid phosphatase type 2B</i>	<i>Hs.405156</i>	-3.77 ± 3.14
<i>PPP2R2B</i>	<i>R55882</i>	<i>Protein phosphatase 2, regulatory subunit B (PR 52), beta isoform</i>	<i>Hs.193825</i>	-1.75 ± 0.17
<i>PPP2R3A</i>	<i>N63863</i>	<i>Protein phosphatase 2, regulatory subunit B (PR 72), alpha isoform and (PR 130), beta isoform</i>	<i>Hs.518155</i>	-1.66 ± 0.13
<i>PPP2R5A</i>	<i>R59164</i>	<i>Protein phosphatase 2, regulatory subunit B, alpha isoform</i>	<i>Hs.497684</i>	-1.88 ± 0.44
<i>PTPRC</i>	<i>H74265</i>	<i>Protein tyrosine phosphatase, receptor type, C</i>	<i>Hs.192039</i>	-1.80 ± 0.42
<i>PTPRF</i>	<i>AA598513</i>	<i>Protein tyrosine phosphatase, receptor type, F</i>	<i>Hs.272062</i>	-1.91 ± 0.42
<i>SSH2</i>	<i>R84636</i>	<i>Slingshot homolog 2</i>	<i>Hs.335205</i>	-1.67 ± 0.24
Peptidases and inhibitors				
<i>ITIH2</i>	<i>R06634</i>	<i>Inter-alpha trypsin inhibitor, H2 polypeptide</i>	<i>Hs.75285</i>	2.67 ± 0.30
<i>MMP3</i>	<i>W51794</i>	<i>Matrix metalloproteinase 3</i>	<i>Hs.375129</i>	12.32 ± 8.47
<i>PLAT</i>	<i>AA453728</i>	<i>Plasminogen activator, tissue</i>	<i>Hs.491582</i>	1.86 ± 0.16
<i>PLAU</i>	<i>AA284668</i>	<i>Plasminogen activator, urokinase</i>	<i>Hs.77274</i>	2.24 ± 0.51
<i>PAPPA</i>	<i>R02529</i>	<i>Pregnancy-associated plasma protein A, pappalysin 1</i>	<i>Hs.643599</i>	1.99 ± 0.24
<i>PSME2</i>	<i>H65395</i>	<i>Proteasome activator subunit 2 (PA28 beta)</i>	<i>Hs.434081</i>	1.77 ± 0.09
<i>SERPINE1</i>	<i>N75719</i>	<i>Serine (or cysteine) proteinase inhibitor, clade E, member 1</i>	<i>Hs.414795</i>	1.69 ± 0.17
<i>SERPINE2</i>	<i>N59721</i>	<i>Serpin peptidase inhibitor, clade E, member 2</i>	<i>Hs.38449</i>	1.87 ± 0.01
<i>SERPINI1</i>	<i>AA115876</i>	<i>Serine (or cysteine) proteinase inhibitor, clade I, member 1</i>	<i>Hs.478153</i>	1.98 ± 0.02
<i>TFPI2</i>	<i>AA399473</i>	<i>Tissue factor pathway inhibitor 2</i>	<i>Hs.438231</i>	12.50 ± 13.13
<i>CPB2</i>	<i>R96561</i>	<i>Carboxypeptidase B2</i>	<i>Hs.512937</i>	-2.15 ± 0.79
<i>CTSE</i>	<i>H94487</i>	<i>Cathepsin E</i>	<i>Hs.1355</i>	-2.27 ± 0.62
<i>H04028</i>	<i>N69322</i>	<i>Matrix metalloproteinase 13</i>	<i>Hs.2936</i>	-2.15 ± 0.76
<i>MMP13</i>	<i>AA031513</i>	<i>Matrix metalloproteinase 7</i>	<i>Hs.2256</i>	-2.55 ± 0.42
<i>MMP7</i>	<i>H50747</i>	<i>Peptidase D</i>	<i>Hs.36473</i>	-1.95 ± 0.33

(1) Gene symbol	(2) Accession	(3) Gene name	(4) Unigene	(5) Fold of changes
<i>P11</i>	<i>H04028</i>	<i>Protease, serine, 22</i>	<i>Hs.997</i>	-1.73 ± 0.30
<i>PEPD</i>	<i>H90815</i>	<i>Serine (or cysteine) proteinase inhibitor, clade A, member 6</i>	<i>Hs.532635</i>	-2.48 ± 0.87
<i>SERPINA6</i>	<i>T62086</i>	<i>Serine (or cysteine) proteinase inhibitor, clade D, member 1</i>	<i>Hs.474270</i>	-1.65 ± 0.13
<i>USP47</i>	<i>H63175</i>	<i>Ubiquitin specific peptidase 47</i>	<i>Hs.567521</i>	-2.03 ± 0.38
Growth factor, cytokines and binding				
AMPH	H06541	Amphiphysin	Hs.592182	2.22 ± 0.74
CCL28	R38459	CC chemokine CCL28	Hs.334633	1.87 ± 0.03
CD34	AA434483	CD34 antigen	Hs.374990	2.21 ± 0.48
CSF3	AI074784	Colony stimulating factor 3	Hs.2233	19.08 ± 2.52
HBEGF	R14663	Diphtheria toxin receptor	Hs.799	2.46 ± 1.15
GTF2IRD1	AA019591	GTF2I repeat domain-containing 1	Hs.647056	2.02 ± 0.23
IGFBP6	AA478724	Insulin-like growth factor binding protein 6	Hs.274313	1.58 ± 0.08
IL1B	AA150507	Interleukin 1, beta	Hs.126256	1.94 ± 0.59
IL32	AA458965	Interleukin 32	Hs.943	1.73 ± 0.04
LIF	R50354	Leukemia inhibitory factor	Hs.2250	3.45 ± 2.74
NRG1	R72075	Neuregulin 1	Hs.453951	2.34 ± 0.74
CCL7	AA040170	Small inducible cytokine A7	Hs.251526	7.15 ± 5.11
CCL13	T64134	Small inducible cytokine subfamily A13	Hs.414629	4.41 ± 2.87
<i>CXCL12</i>	<i>AA447115</i>	<i>Chemokine (C-X-C motif) ligand 12</i>	<i>Hs.522891</i>	-1.85 ± 0.53
<i>CXCL9</i>	<i>AA131406</i>	<i>Chemokine (C-X-C motif) ligand 9</i>	<i>Hs.77367</i>	-2.05 ± 0.23
<i>C5</i>	<i>N73030</i>	<i>Complement component 5</i>	<i>Hs.494997</i>	-2.1 ± 0.37
<i>IGFBP1</i>	<i>AA233079</i>	<i>Insulin-like growth factor binding protein 1</i>	<i>Hs.401316</i>	-1.74 ± 0.18
<i>IGFBP2</i>	<i>H79047</i>	<i>Insulin-like growth factor binding protein 2</i>	<i>Hs.438102</i>	-2.11 ± 0.73
<i>IGFBP3</i>	<i>AA598601</i>	<i>Insulin-like growth factor binding protein 3</i>	<i>Hs.450230</i>	-2.34 ± 0.24
<i>IL6R</i>	<i>T97204</i>	<i>Interleukin 6 receptor</i>	<i>Hs.135087</i>	-2.34 ± 1.12
<i>MUC1</i>	<i>AA488073</i>	<i>Mucin 1, transmembrane</i>	<i>Hs.89603</i>	-1.88 ± 0.46
<i>PGM5P1</i>	<i>H12279</i>	<i>Phosphoglucomutase 5</i>	<i>Hs.178400</i>	-2.28 ± 1.07
<i>TNFRSF25</i>	<i>W76376</i>	<i>Tumor necrosis factor receptor superfamily, member 25</i>	<i>Hs.462529</i>	-2.03 ± 0.58
Receptor activity				
ACVR2B	R68237	ACVR2B: Activin A receptor, type IIB	Hs.517775	2.26 ± 1.02
CR1L	T66824	Complement component receptor 1-like	Hs.334019	1.72 ± 0.07
EPHA1	N90246	EphA1	Hs.89839	1.66 ± 0.16
PTGER4	AA019996	Prostaglandin E receptor 4	Hs.199248	1.72 ± 0.10
LRPAP1	AA486313	Low density lipoprotein-related protein-associated protein 1	Hs.533136	1.62 ± 0.04
RYR2	R15791	Ryanodine receptor 2	Hs.109514	1.57 ± 0.02
PROCR	T47442	Protein C receptor, endothelial	Hs.82353	1.56 ± 0.01
TNFRSF12A	R33355	Tumor necrosis factor receptor superfamily, member 12A	Hs.355899	3.45 ± 1.92
<i>ANTXR1</i>	<i>H58644</i>	<i>Anthrax toxin receptor 1</i>	<i>Hs.165859</i>	-1.82 ± 0.32
<i>AY114160.1</i>	<i>N57964</i>	<i>Chemokine (C-C motif) receptor 6</i>	<i>Hs.46468</i>	-2.27 ± 0.57
<i>CCR6</i>	<i>H60460</i>	<i>CD302 antigen</i>	<i>Hs.130014</i>	-2.12 ± 0.54
<i>CD302</i>	<i>AA485795</i>	<i>Ephrin-B3</i>	<i>Hs.26988</i>	-1.91 ± 0.19

(1) Gene symbol	(2) Accession	(3) Gene name	(4) Unigene	(5) Fold of changes
<i>EFNB3</i>	AA456376	Coagulation factor II (thrombin) receptor	Hs.482562	-2.47 ± 0.76
<i>GABRP</i>	AA102670	Gamma-aminobutyric acid (GABA) A receptor, pi	Hs.26225	-1.91 ± 0.33
<i>GRIA1</i>	H23378	Glutamate receptor, ionotropic, AMPA 1	Hs.519693	-1.80 ± 0.04
<i>ITPR2</i>	AA479093	Inositol 1,4,5-triphosphate receptor, type 2	Hs.512235	-1.88 ± 0.49
<i>IGF2R</i>	T62547	Insulin-like growth factor 2 receptor	Hs.487062	-1.56 ± 0.06
<i>ITGA10</i>	H44722	Integrin, alpha 10	Hs.158237	-2.01 ± 0.70
<i>ITGB8</i>	W56709	Integrin, beta 8	Hs.592171	-3.29 ± 1.22
<i>KLRC2</i>	AA191156	Killer cell lectin-like receptor subfamily C, member 2	Hs.74082	-1.71 ± 0.13
<i>KIT</i>	N24824	V-kit Hardy-Zuckerman 4 feline sarcoma viral oncogene homolog, Kit receptor	Hs.479754	-1.70 ± 0.14
<i>PLA2R1</i>	R91516	Phospholipase A2 receptor 1, 180 kDa	Hs.410477	-2.22 ± 0.82
Transporters				
ATP6V1B1	R73402	ATPase, H ⁺ transporting, lysosomal, beta 1	Hs.64173	2.08 ± 0.17
ABCC3	AA429895	ATP-binding cassette, sub-family C, member 3	Hs.463421	3.96 ± 2.68
LIPC	N80949	Lipase, hepatic	Hs.188630	1.82 ± 0.35
SLC15A2	AA425352	Solute carrier family 15 (H ⁺ /peptide transporter), member 2	Hs.518089	6.00 ± 4.28
SLC35D1	W16916	Solute carrier family 35 (UDP-glucuronic acid/UDP-N-acetylgalactosamine dual transporter), member D1	Hs.213642	2.26 ± 0.19
SORL1	AA424516	sortilin-related receptor, L(DLR class) A repeats-containing	Hs.368592	2.21 ± 0.40
STARD4	H11369	START domain containing 4, sterol regulated	Hs.93842	1.95 ± 0.02
TAP1	AA487637	Transporter 1, ATP-binding cassette, sub-family B	Hs.352018	1.64 ± 0.03
TLOC1	AA450205	Translocation protein 1	Hs.529591	1.93 ± 0.53
KCNAB2	H14383	Potassium voltage-gated channel, shaker-related subfamily, beta member 2	Hs.440497	1.55 ± 0.01
<i>ABCB1</i>	AA455911	ATP-binding cassette, sub-family B, member 1	Hs.489033	-1.69 ± 0.26
<i>ABCB10</i>	R83875	ATP-binding cassette, sub-family B, member 10	Hs.17614	-1.97 ± 0.39
<i>FYCO1</i>	R11564	FYVE and coiled-coil domain containing 1	Hs.200227	-2.09 ± 0.40
<i>SLC6A1</i>	H61935	Solute carrier family 6, member 1	Hs.443874	-2.09 ± 0.76
Signaling molecules				
CFLAR	N94588	CASP8 and FADD-like apoptosis regulator	Hs.390736	1.79 ± 0.39
GTPBP2	T67069	GTP binding protein 2	Hs.485449	4.07 ± 1.71
LRRFIP2	W30810	Leucine rich repeat (in FLII) interacting protein 2	Hs.475319	2.77 ± 0.90
MX1	AA456886	Myxovirus resistance 1	Hs.517307	4.10 ± 0.74
MX2	AA286908	Myxovirus resistance 2	Hs.926	3.18 ± 0.14
NFKBIA	W55872	I-kappa-B-alpha	Hs.81328	2.23 ± 0.83
NKIRAS2	R63172	I-kappa-B-interacting Ras-like protein 2	Hs.632252	1.85 ± 0.28
RAB25	W25368	RAB25, member RAS oncogene family	Hs.632469	2.06 ± 0.47
RAB36	H69004	RAB36, member RAS oncogene family	Hs.369557	1.76 ± 0.05
RAB3IP	W96273	RAB3A interacting protein	Hs.258209	1.89 ± 0.01
RANGAP1	AA026631	Ran GTPase activating protein 1	Hs.183800	1.99 ± 0.33
RIT1	AA027840	Ras-like without CAAX 1	Hs.491234	2.06 ± 0.64
RRAS2	R21415	Related RAS viral (r-ras) oncogene homolog 2	Hs.502004	1.66 ± 0.05
SH3BGR	N52254	SH3 domain binding glutamic acid-rich protein	Hs.473847	4.47 ± 2.12

(1) Gene symbol	(2) Accession	(3) Gene name	(4) Unigene	(5) Fold of changes
STC2	R20886	Stanniocalcin 2	Hs.233160	3.91 ± 3.69
TRAF3	AA504259	TNF receptor-associated factor 3	Hs.510528	2.13 ± 0.10
TRH	AA069596	Thyrotropin-releasing hormone	Hs.182231	1.77 ± 0.32
<i>BIRC3</i>	<i>H48706</i>	<i>Baculoviral IAP repeat-containing 3</i>	<i>Hs.127799</i>	<i>-1.74 ± 0.01</i>
<i>CEACAM6</i>	<i>AA054073</i>	<i>Carcinoembryonic antigen-related cell adhesion molecule 6</i>	<i>Hs.466814</i>	<i>-1.81 ± 0.16</i>
<i>FRZB</i>	<i>W58032</i>	<i>Frizzled-related protein</i>	<i>Hs.128453</i>	<i>-2.37 ± 0.49</i>
<i>GBP2</i>	<i>W77927</i>	<i>Guanylate binding protein 2, interferon-inducible</i>	<i>Hs.386567</i>	<i>-2.77 ± 0.58</i>
<i>GEM</i>	<i>AA418077</i>	<i>GTP-binding protein overexpressed in skeletal muscle</i>	<i>Hs.345139</i>	<i>-1.61 ± 0.01</i>
<i>GNG2</i>	<i>T80932</i>	<i>Guanine nucleotide binding protein (G protein), gamma 2</i>	<i>Hs.187772</i>	<i>-3.19 ± 1.20</i>
<i>IQGAP1</i>	<i>AA598496</i>	<i>IQ motif containing GTPase activating protein 1</i>	<i>Hs.430551</i>	<i>-2.68 ± 1.44</i>
<i>KRAS</i>	<i>N95249</i>	<i>v-Ki-ras2 Kirsten rat sarcoma viral oncogene homolog</i>	<i>Hs.505033</i>	<i>-2.21 ± 0.54</i>
<i>LETM1</i>	<i>AA417654</i>	<i>leucine zipper-EF-hand containing transmembrane protein 1</i>	<i>Hs.120165</i>	<i>-2.01 ± 0.65</i>
<i>MCF2</i>	<i>H05800</i>	<i>MCF.2 cell line derived transforming sequence</i>	<i>Hs.387262</i>	<i>-2.69 ± 0.85</i>
<i>PLCL1</i>	<i>AA411387</i>	<i>phospholipase C-like 1</i>	<i>Hs.153322</i>	<i>-2.57 ± 0.57</i>
<i>PSD3</i>	<i>R98905</i>	<i>Pleckstrin and Sec7 domain containing 3</i>	<i>Hs.434255</i>	<i>-2.81 ± 1.66</i>
<i>ARHGEF6</i>	<i>AA236617</i>	<i>Rac/Cdc42 guanine exchange factor 6</i>	<i>Hs.522795</i>	<i>-1.93 ± 0.23</i>
<i>RHOBTB3</i>	<i>N52517</i>	<i>Rho-related BTB domain containing 3</i>	<i>Hs.445030</i>	<i>-2.32 ± 0.93</i>
<i>SOS1</i>	<i>H64324</i>	<i>Son of sevenless homolog 1</i>	<i>Hs.278733</i>	<i>-2.27 ± 0.42</i>
<i>SOS2</i>	<i>R78735</i>	<i>Son of sevenless homolog 2</i>	<i>Hs.291533</i>	<i>-1.75 ± 0.21</i>
<i>TSPAN8</i>	<i>AA045698</i>	<i>Tetraspanin 8</i>	<i>Hs.170563</i>	<i>-1.83 ± 0.17</i>
<i>WNT2</i>	<i>T99653</i>	<i>Wingless-type MMTV integration site family member 2</i>	<i>Hs.567356</i>	<i>-3.14 ± 1.00</i>
Kinase activity				
DGKA	AA456900	Diacylglycerol kinase, alpha	Hs.524488	1.87 ± 0.36
DYRK3	H62028	Dual-specificity tyrosine phosphorylation regulated kinase 3	Hs.164267	2.14 ± 0.92
MAP2K6	H07920	Mitogen-activated protein kinase kinase 6	Hs.463978	1.72 ± 0.03
MAST1	AA479623	Microtubule associated serine/threonine kinase 1	Hs.227489	1.63 ± 0.10
MAST4	AA418846	Microtubule associated serine/threonine kinase family member 4	Hs.133539	1.67 ± 0.04
PCTK3	AA398949	PCTAIRE protein kinase 3	Hs.445402	1.7 ± 0.00
PFKP	R38433	Phosphofructokinase, platelet	Hs.26010	1.65 ± 0.07
PRKCZ	R24258	Protein kinase C, zeta	Hs.496255	1.98 ± 0.45
SNF1LK2	H90161	SNF1-like kinase 2	Hs.555922	2.64 ± 0.59
AURKA	R19158	Serine/threonine kinase 15	Hs.250822	2.62 ± 0.49
STK38	H47863	Serine/threonine kinase 38	Hs.409578	2.39 ± 0.43
<i>FYN</i>	<i>H91826</i>	<i>FYN oncogene related to SRC, FGR, YES</i>	<i>Hs.390567</i>	<i>-2.42 ± 1.23</i>
<i>MAPK7</i>	<i>H39192</i>	<i>Mitogen-activated protein kinase 7</i>	<i>Hs.150136</i>	<i>-2.97 ± 1.55</i>
<i>MERTK</i>	<i>AA436591</i>	<i>C-mer proto-oncogene tyrosine kinase</i>	<i>Hs.306178</i>	<i>-1.79 ± 0.07</i>
<i>PIK3C2G</i>	<i>T66837</i>	<i>Phosphoinositide-3-kinase, class 2, gamma</i>	<i>Hs.22500</i>	<i>-2.39 ± 0.85</i>
<i>PIP5K2A</i>	<i>H93068</i>	<i>Phosphatidylinositol-4-phosphate 5-kinase, type II, alpha</i>	<i>Hs.588901</i>	<i>-2.19 ± 0.57</i>
<i>PRKCB1</i>	<i>AA479102</i>	<i>Protein kinase C, beta 1</i>	<i>Hs.460355</i>	<i>-1.73 ± 0.18</i>
<i>PRKCG</i>	<i>R89715</i>	<i>Protein kinase C, gamma</i>	<i>Hs.2890</i>	<i>-2.02 ± 0.58</i>
<i>STK3</i>	<i>AA464628</i>	<i>Serine/threonine kinase 3</i>	<i>Hs.492333</i>	<i>-1.80 ± 0.23</i>

(1) Gene symbol	(2) Accession	(3) Gene name	(4) Unigene	(5) Fold of changes
<i>STK17A</i>	<i>H65942</i>	<i>Serine/threonine kinase 17a</i>	<i>Hs.268887</i>	-2.43 ± 0.46
Structural				
CALD1	N95107	caldesmon 1	Hs.490203	2.01 ± 0.68
DST	H44784	Dystonin	Hs.631992	2.23 ± 0.32
DSP	H90899	Desmoplakin	Hs.519873	1.65 ± 0.03
EVPL	AA029418	Envoplakin	Hs.500635	2.20 ± 0.28
INA	AA448015	Internexin neuronal intermediate filament protein, alpha	Hs.500916	1.70 ± 0.08
VCL	AA486728	Vinculin	Hs.500101	2.70 ± 1.12
<i>A2M</i>	<i>H06516</i>	<i>Alpha-2-macroglobulin</i>	<i>Hs.212838</i>	-3.07 ± 0.39
<i>COL14A1</i>	<i>AA167222</i>	<i>Collagen, type XIV, alpha 1</i>	<i>Hs.409662</i>	-3.16 ± 0.92
<i>COL1A2</i>	<i>AA490172</i>	<i>Collagen, type I, alpha 2</i>	<i>Hs.489142</i>	-2.28 ± 1.09
<i>CTNND2</i>	<i>H04985</i>	<i>Catenin (cadherin-associated protein), delta 2</i>	<i>Hs.314543</i>	-1.66 ± 0.20
<i>DST</i>	<i>W00789</i>	<i>Dystonin</i>	<i>Hs.485616</i>	-1.98 ± 0.03
<i>FBLN2</i>	<i>AA452981</i>	<i>Fibulin 2</i>	<i>Hs.198862</i>	-2.7 ± 1.67
<i>LUM</i>	<i>AA453712</i>	<i>Lumican</i>	<i>Hs.406475</i>	-3.47 ± 2.58
<i>MBP</i>	<i>H17696</i>	<i>Myelin basic protein</i>	<i>Hs.551713</i>	-2.16 ± 0.51
<i>MYH10</i>	<i>AA490477</i>	<i>Myosin, heavy polypeptide 10, non-muscle</i>	<i>Hs.16355</i>	-1.95 ± 0.66
<i>MYLIP</i>	<i>AA486836</i>	<i>myosin regulatory light chain interacting protein</i>	<i>Hs.484738</i>	-1.77 ± 0.13
<i>THBS1</i>	<i>AA464630</i>	<i>Thrombospondin 1</i>	<i>Hs.164226</i>	-3.53 ± 2.73
Protein binding				
APBA2	R55789	Amyloid beta precursor protein-binding, family A, member 2	Hs.525718	1.86 ± 0.14
BCL2	W63749	Bcl-2	Hs.150749	1.93 ± 0.52
CCND1	AA487700	Cyclin D1	Hs.523852	1.94 ± 0.31
CCT2	N38959	Chaperonin containing TCP1, subunit 2	Hs.189772	1.67 ± 0.01
INTS7	N80458	DKFZP434B168 protein	Hs.369285	2.21 ± 0.40
ETF1	AA456664	Eukaryotic translation termination factor 1	Hs.483494	1.63 ± 0.10
ITGA2	AA463610	Integrin, alpha 2	Hs.482077	2.13 ± 0.34
ITGB8	R74357	Integrin, beta 8	Hs.592171	1.75 ± 0.28
NCSTN	R96527	Nicastrin	Hs.517249	2.25 ± 0.63
PHLDA1	AA258396	Pleckstrin homology-like domain, family A, member 1	Hs.484885	2.13 ± 0.49
RP2	W00899	Retinitis pigmentosa 2	Hs.44766	1.65 ± 0.07
PCGF3	R06308	Ring finger protein 3	Hs.144309	1.55 ± 0.06
RNF10	H73586	Ring finger protein 10	Hs.442798	1.79 ± 0.40
SAC3D1	W95346	SAC3 domain containing 1	Hs.23642	2.06 ± 0.18
TNFAIP3	AA476272	Tumor necrosis factor alpha-induced protein 3	Hs.591338	2.36 ± 1.09
UBE2D3	R91710	Ubiquitin-conjugating enzyme E2D 3	Hs.518773	2.10 ± 0.62
UBE2I	AA487197	Ubiquitin-conjugating enzyme E2I	Hs.302903	3.62 ± 0.12
<i>YWHAH</i>	<i>N74377</i>	<i>14-3-3 protein eta</i>	<i>Hs.226755</i>	-2.14 ± 0.89
<i>AKAP12</i>	<i>AA478542</i>	<i>A kinase (PRKA) anchor protein (gravin) 12</i>	<i>Hs.371240</i>	-1.68 ± 0.13
<i>PAR3beta</i>	<i>R99773</i>	<i>Amyotrophic lateral sclerosis 2 chromosome region, candidate 19</i>	<i>Hs.271903</i>	-1.90 ± 0.46
<i>CDH11</i>	<i>H96738</i>	<i>Cadherin 11, type 2, OB-cadherin</i>	<i>Hs.116471</i>	-2.06 ± 0.74

(1) Gene symbol	(2) Accession	(3) Gene name	(4) Unigene	(5) Fold of changes
<i>CHL1</i>	<i>R40400</i>	<i>Cell adhesion molecule with homology to L1CAM</i>	<i>Hs.148909</i>	-1.83 ± 0.14
<i>CUL4A</i>	<i>R02425</i>	<i>Cullin 4A</i>	<i>Hs.339735</i>	-1.77 ± 0.33
	<i>AA133797</i>	<i>Deleted in azoospermia</i>	<i>Hs.522868</i>	-1.73 ± 0.03
<i>DAZAP2</i>	<i>R19889</i>	<i>DAZ associated protein 2</i>	<i>Hs.369761</i>	-1.66 ± 0.01
<i>EGFLAM</i>	<i>R08141</i>	<i>EGF-like, fibronectin type III and laminin G domains</i>	<i>Hs.20103</i>	-2.21 ± 0.57
<i>FANCC</i>	<i>H62396</i>	<i>Fanconi anemia, complementation group C</i>	<i>Hs.494529</i>	-1.94 ± 0.56
<i>FYB</i>	<i>N64862</i>	<i>FYN-binding protein</i>	<i>Hs.370503</i>	-2.13 ± 0.05
<i>MTMR3</i>	<i>R11490</i>	<i>Nucleoprotein TPR, Translocated promoter region (to activated MET oncogene)</i>	<i>Hs.279640</i>	-2.42 ± 1.29
<i>NAP1L4</i>	<i>H92347</i>	<i>Nucleosome assembly protein 1-like 4</i>	<i>Hs.501684</i>	-1.67 ± 0.09
<i>NCF1</i>	<i>AA459308</i>	<i>Neutrophil cytosolic factor 1,</i>	<i>Hs.520943</i>	-2.08 ± 0.55
<i>POSTN</i>	<i>AA598653</i>	<i>Periostin, osteoblast specific factor</i>	<i>Hs.136348</i>	-3.13 ± 2.18
<i>PRAME</i>	<i>AA598817</i>	<i>Preferentially expressed antigen in melanoma</i>	<i>Hs.30743</i>	-1.71 ± 0.14
<i>RTN4</i>	<i>N68565</i>	<i>Reticulon 4</i>	<i>Hs.429581</i>	-1.72 ± 0.02
<i>SELL</i>	<i>H00756</i>	<i>Selectin L</i>	<i>Hs.82848</i>	-2.03 ± 0.51
<i>SNX19</i>	<i>AA040424</i>	<i>Sorting nexin 19</i>	<i>Hs.444024</i>	-5.93 ± 6.19
<i>TJP2</i>	<i>W31983</i>	<i>Tight junction protein 2</i>	<i>Hs.50382</i>	-2.73 ± 0.99
<i>TNC</i>	<i>T69489</i>	<i>Tenascin C</i>	<i>Hs.143250</i>	-1.80 ± 0.02
<i>UBE2V1</i>	<i>H69048</i>	<i>Ubiquitin-conjugating enzyme E2 variant 1</i>	<i>Hs.420529</i>	-2.42 ± 0.89
<i>VCAM1</i>	<i>H07071</i>	<i>Vascular cell adhesion molecule 1</i>	<i>Hs.109225</i>	-2.50 ± 0.60
Transcription related				
<i>MPPED2</i>	<i>AA020011</i>	<i>Chromosome 11 open reading frame 8</i>	<i>Hs.289795</i>	1.77 ± 0.23
<i>DPF3</i>	<i>R02268</i>	<i>D4, zinc and double PHD fingers, family 3</i>	<i>Hs.162868</i>	2.07 ± 0.28
<i>FLJ23311</i>	<i>W04152</i>	<i>E2F transcription factor 8</i>	<i>Hs.523526</i>	1.87 ± 0.32
<i>FOXC1</i>	<i>W94714</i>	<i>Forkhead box C1</i>	<i>Hs.348883</i>	2.06 ± 0.18
<i>HIP2</i>	<i>H53038</i>	<i>Huntingtin interacting protein 2</i>	<i>Hs.50308</i>	1.62 ± 0.03
<i>HNRPD</i>	<i>H11069</i>	<i>Heterogeneous nuclear ribonucleoprotein D</i>	<i>Hs.480073</i>	1.84 ± 0.05
<i>JARID1A</i>	<i>AA460756</i>	<i>Jumonji, AT rich interactive domain 1A</i>	<i>Hs.76272</i>	2.37 ± 1.05
<i>JARID2</i>	<i>N73555</i>	<i>Jumonji, AT rich interactive domain 2</i>	<i>Hs.269059</i>	3.62 ± 1.67
<i>JUN</i>	<i>W96155</i>	<i>V-jun avian sarcoma virus 17 oncogene homolog</i>	<i>Hs.525704</i>	1.73 ± 0.23
<i>MYC</i>	<i>W87741</i>	<i>V-myc myelocytomatosis viral oncogene homolog</i>	<i>Hs.202453</i>	1.96 ± 0.20
<i>NFE2</i>	<i>H59000</i>	<i>Nuclear factor, 45kD (NF-E2)</i>	<i>Hs.75643</i>	1.70 ± 0.20
<i>NR4A2</i>	<i>AA598611</i>	<i>Nuclear receptor subfamily 4, group A, member 2</i>	<i>Hs.563344</i>	2.50 ± 0.94
<i>NR4A3</i>	<i>H37761</i>	<i>Nuclear receptor subfamily 4, group A, member 3</i>	<i>Hs.279522</i>	2.37 ± 0.46
<i>REL</i>	<i>N32146</i>	<i>V-rel reticuloendotheliosis viral oncogene homolog</i>	<i>Hs.631886</i>	1.77 ± 0.17
<i>STAT1</i>	<i>AA486367</i>	<i>Signal transducer and activator of transcription 1, 91kD</i>	<i>Hs.470943</i>	2.14 ± 0.48
<i>TAL1</i>	<i>R97066</i>	<i>T-cell acute lymphocytic leukemia 1</i>	<i>Hs.73828</i>	2.64 ± 0.28
<i>TRIM22</i>	<i>AA083407</i>	<i>Tripartite motif-containing 22</i>	<i>Hs.501778</i>	1.60 ± 0.03
<i>TRIM25</i>	<i>N73575</i>	<i>Tripartite motif-containing 25</i>	<i>Hs.528952</i>	1.61 ± 0.06
<i>TSC22D2</i>	<i>R62373</i>	<i>TSC22 domain family member 2</i>	<i>Hs.52526</i>	1.78 ± 0.09
<i>USF2</i>	<i>AA489017</i>	<i>Upstream transcription factor 2, c-fos interacting</i>	<i>Hs.454534</i>	1.74 ± 0.11
<i>ARID5B</i>	<i>T77812</i>	<i>AT rich interactive domain 5B (MRF1-like)</i>	<i>Hs.535297</i>	-2.23 ± 0.39

(1) Gene symbol	(2) Accession	(3) Gene name	(4) Unigene	(5) Fold of changes
<i>BMI1</i>	AA478036	<i>B lymphoma Mo-MLV insertion region</i>	Hs.496613	-1.62 ± 0.15
<i>ELF2</i>	AA453714	<i>E74-like factor 2</i>	Hs.480763	-1.60 ± 0.02
<i>MEF2C</i>	AA234897	<i>MADS box transcription enhancer factor 2C</i>	Hs.444409	-1.86 ± 0.08
<i>MTA1</i>	N71159	<i>Metastasis associated 1</i>	Hs.525629	-1.53 ± 0.02
<i>MYCN</i>	R66447	<i>V-myc avian myelocytomatosis viral related oncogene, neuroblastoma derived</i>	Hs.25960	-1.84 ± 0.16
<i>MYST4</i>	AA057313	<i>MYST histone acetyltransferase 4</i>	Hs.35758	-3.19 ± 1.02
<i>NR2F1</i>	AA452909	<i>Nuclear receptor subfamily 2, group F, member 1</i>	Hs.519445	-1.95 ± 0.33
<i>PBX1</i>	H68663	<i>Pre-B-cell leukemia transcription factor 1</i>	Hs.493096	-1.76 ± 0.07
<i>PCAF</i>	W00975	<i>P300/CBP-associated factor</i>	Hs.533055	-2.25 ± 0.08
<i>PITX2</i>	T64905	<i>Paired-like homeodomain transcription factor 2</i>	Hs.643588	-1.69 ± 0.04
<i>PLAG1</i>	AA418251	<i>Pleiomorphic adenoma gene 1</i>	Hs.14968	-1.64 ± 0.04
<i>POLR2A</i>	AA479052	<i>Polymerase (RNA) II (DNA directed) polypeptide A (220kD)</i>	Hs.270017	-2.32 ± 1.13
<i>PRDM2</i>	W76648	<i>PR domain containing 2, with ZNF domain</i>	Hs.371823	-1.75 ± 0.12
<i>RUNX1T1</i>	H37846	<i>Runt-related transcription factor 1</i>	Hs.368431	-2.11 ± 0.60
<i>SMARCA3</i>	AA459632	<i>SWI/SNF related, matrix associated, actin dependent regulator of chromatin, subfamily a, member 3</i>	Hs.3068	-1.82 ± 0.16
<i>SNAI2</i>	H57309	<i>snail homolog 2</i>	Hs.360174	-2.35 ± 0.61
<i>SOX9</i>	AA400739	<i>SRY -box 9</i>	Hs.647409	-2.04 ± 0.15
<i>SP3</i>	W32135	<i>Sp3 transcription factor</i>	Hs.531587	-1.95 ± 0.66
<i>TCF12</i>	N51828	<i>Transcription factor 12</i>	Hs.511504	-1.80 ± 0.35
<i>TCF7L2</i>	N76867	<i>Transcription factor 7-like 2</i>	Hs.593995	-2.02 ± 0.16
<i>TCF8</i>	H46553	<i>Transcription factor 8</i>	Hs.124503	-2.62 ± 1.06
<i>TFAP4</i>	AA284693	<i>Transcription factor AP-4</i>	Hs.587500	-1.62 ± 0.10
<i>TTF1</i>	T60168	<i>Thyroid transcription factor 1</i>	Hs.94367	-1.74 ± 0.16
<i>ZFP36L1</i>	AA723035	<i>zinc finger protein 36, C3H type-like 1</i>	Hs.85155	-1.82 ± 0.19
DNA/RNA/nucleotide binding				
<i>ABL1</i>	R00766	<i>V-abl Abelson murine leukemia viral oncogene homolog 1</i>	Hs.431048	1.88 ± 0.45
<i>ADARB1</i>	AA489331	<i>Adenosine deaminase, RNA-specific, B1</i>	Hs.474018	1.72 ± 0.12
<i>ARF4L</i>	H28952	<i>ADP-ribosylation factor 4-like</i>	Hs.183153	2.80 ± 0.43
<i>DDB2</i>	AA406449	<i>Damage-specific DNA binding protein 2</i>	Hs.651197	1.57 ± 0.09
<i>DDX26B</i>	T99650	<i>DEAD/H (Asp-Glu-Ala-Asp/His) box polypeptide 26B</i>	Hs.496829	2.24 ± 0.97
<i>EIF2B5</i>	R54818	<i>Eukaryotic translation initiation factor 2B, subunit 5</i>	Hs.283551	1.80 ± 0.32
<i>HIST1H1C</i>	T66816	<i>Histone cluster 1, H1c</i>	Hs.7644	3.32 ± 1.36
<i>HIST1H2AC</i>	AA453105	<i>Histone cluster 1, H2ac</i>	Hs.484950	1.96 ± 0.37
<i>HIST1H2BD</i>	N33927	<i>Histone cluster 1, H2bd</i>	Hs.130853	1.88 ± 0.22
<i>HIST2H2BE</i>	AA456695	<i>Histone cluster 2, H2be</i>	Hs.2178	2.14 ± 0.42
<i>MRPL3</i>	H05820	<i>Mitochondrial ribosomal protein L3</i>	Hs.205163	1.77 ± 0.04
<i>PAPOLG</i>	R62241	<i>Poly(A) polymerase gamma</i>	Hs.387471	2.1 ± 0.38
<i>PEG10</i>	H51765	<i>Paternally expressed 10</i>	Hs.147492	1.72 ± 0.08
<i>RBM38</i>	AA459588	<i>RNA binding motif protein 38</i>	Hs.236361	1.68 ± 0.16
<i>TOP1</i>	R60160	<i>Topoisomerase (DNA) I</i>	Hs.592136	2.05 ± 0.07

(1) Gene symbol	(2) Accession	(3) Gene name	(4) Unigene	(5) Fold of changes
ZCCHC2	N54297	Zinc finger, CCHC domain containing 2	Hs.114191	2.10 ± 0.70
ZNF662	N91317	Zinc finger protein 662	Hs.293388	2.33 ± 0.94
ZNF587	H80423	Zinc finger protein 587	Hs.288995	1.81 ± 0.10
<i>CCAR1</i>	<i>W05026</i>	<i>Cell division cycle and apoptosis regulator 1</i>	<i>Hs.49853</i>	<i>-2.90 ± 1.81</i>
<i>FXR1</i>	<i>N79708</i>	<i>Fragile X mental retardation, autosomal homolog 1</i>	<i>Hs.478407</i>	<i>-1.84 ± 0.46</i>
<i>IGF2BP2</i>	<i>W00973</i>	<i>Insulin-like growth factor 2 mRNA binding protein 2</i>	<i>Hs.35354</i>	<i>-2.01 ± 0.32</i>
<i>KIF21B</i>	<i>H14513</i>	<i>Kinesin family member 21B</i>	<i>Hs.169182</i>	<i>-2.45 ± 1.27</i>
<i>KIF6</i>	<i>N74348</i>	<i>Kinesin family member 6</i>	<i>Hs.588202</i>	<i>-1.84 ± 0.17</i>
<i>MRPS5</i>	<i>R26977</i>	<i>mitochondrial ribosomal protein S5</i>	<i>Hs.355664</i>	<i>-2.2 ± 0.93</i>
<i>SFRS11</i>	<i>H56944</i>	<i>Splicing factor, arginine/serine-rich 11</i>	<i>Hs.479693</i>	<i>-2.11 ± 0.30</i>
<i>TIA1</i>	<i>AA427663</i>	<i>TIA1 cytotoxic granule-associated RNA-binding protein</i>	<i>Hs.516075</i>	<i>-1.99 ± 0.59</i>
<i>ZFHX4</i>	<i>N45083</i>	<i>Zinc finger homeodomain 4</i>	<i>Hs.458973</i>	<i>-2.33 ± 0.78</i>
Miscellaneous				
MMACHC	T67050	DKFZP5641122 protein	Hs.13024	1.87 ± 0.46
DSCR1L2	R27172	Down syndrome critical region gene 1-like 2	Hs.399958	2.13 ± 0.80
DYNC1LI2	AA454959	Dynein, cytoplasmic, light intermediate polypeptide 2	Hs.369068	2.33 ± 0.80
DKFZp313A2432AF527534.1		Hypothetical protein DKFZp313A2432	Hs.349096	2.06 ± 0.75
PFKFB1	T67104	Purinergic receptor P2Y, G-protein coupled, 13	Hs.444304	2.12 ± 0.46
S100A2	AA458884	S100 calcium-binding protein A2	Hs.516484	1.85 ± 0.02
TTLL12	R44546	KIAA0153 protein	Hs.517670	2.71 ± 0.26
KIAA1571	R68133	KIAA1571 protein	Hs.110489	1.85 ± 0.31
THAP6	N24268	THAP domain containing 6	Hs.479971	2.77 ± 1.42
UROS	T82469	Uroporphyrinogen III synthase	Hs.501376	1.84 ± 0.27
<i>ADAMTSL4</i>	<i>R96552</i>	<i>ADAMTS-like 4</i>	<i>Hs.516243</i>	<i>-2.86 ± 1.90</i>
<i>BAT2D1</i>	<i>R00395</i>	<i>BAT2 domain containing 1</i>	<i>Hs.494614</i>	<i>-1.74 ± 0.09</i>
<i>CCAR1</i>	<i>W05026</i>	<i>Cell division cycle and apoptosis regulator 1</i>	<i>Hs.49853</i>	<i>-2.90 ± 1.81</i>
<i>CCDC35</i>	<i>T85902</i>	<i>Coiled-coil domain containing 35</i>	<i>Hs.135119</i>	<i>-1.73 ± 0.16</i>
<i>DLL1</i>	<i>R41685</i>	<i>Delta-like 1</i>	<i>Hs.379912</i>	<i>-1.82 ± 0.46</i>
<i>FBXO3</i>	<i>T97183</i>	<i>F-box protein 3</i>	<i>Hs.406787</i>	<i>-1.88 ± 0.24</i>
<i>KIAA0423</i>	<i>N50014</i>	<i>KIAA0423 protein</i>	<i>Hs.371078</i>	<i>-1.98 ± 0.42</i>
<i>LDB2</i>	<i>H74106</i>	<i>LIM domain binding 2</i>	<i>Hs.23748</i>	<i>-2.70 ± 1.60</i>
<i>MAL</i>	<i>AA227594</i>	<i>Mal, T-cell differentiation protein</i>	<i>Hs.80395</i>	<i>-1.62 ± 0.01</i>
<i>PAN3</i>	<i>R68381</i>	<i>PABP1-dependent poly A-specific ribonuclease subunit PAN3</i>	<i>Hs.369984</i>	<i>-1.78 ± 0.28</i>
<i>SAPS3</i>	<i>R10015</i>	<i>SAPS domain family, member 3</i>	<i>Hs.503022</i>	<i>-1.61 ± 0.03</i>
<i>TBC1D7</i>	<i>H91404</i>	<i>TBC1 domain family, member 7</i>	<i>Hs.484678</i>	<i>-1.89 ± 0.30</i>
<i>TRIB2</i>	<i>AA458653</i>	<i>Tribbles homolog 2</i>	<i>Hs.467751</i>	<i>-2.85 ± 2.04</i>
<i>VGLL3</i>	<i>R62289</i>	<i>Vestigial like 3</i>	<i>Hs.435013</i>	<i>-2.73 ± 1.60</i>

HDFs were treated with 600 μ M H₂O₂ for 2 h and were placed in fresh culture medium for 72 hr recovery before harvesting RNA for cDNA microarray analyses (see Materials and methods). The data indicate the averages and standard deviations of fold changes from at least two independent experiments. The fold of increase or decrease (negative numbers in italic) for each gene was determined by GeneSpring 5.0 software as statistically significant changes for at least two out of three independent experiments. The column in the table represents (1) Gene symbol, (2) Accession number, (3) common name of the gene, (4) Unigene number, (5) fold of change for increase and decrease. Many genes can be placed

into multiple functional categories. In the case a gene has multiple functions, it is placed under the category of its most commonly recognized function

Author Manuscript

Author Manuscript

Author Manuscript

Author Manuscript